Understanding the complexity of TGF-beta signaling in cancer

Marvin, D.L.

CHAPTER 8

TRAF4 Inhibits Bladder Cancer Progression by Promoting BMP/SMAD Signaling

Prasanna Vasudevan Iyengar[1,2], Dieuwke Louise Marvin[1,2], Dilraj Lama[3,4], Tuan Zea Tan[5], Sudha Suriyamurthy[1,2], Feng Xie[6,7], Maarten van Dinther[1,2], Hailiang Mei[8], Chandra Shekhar Verma[4,9,10], Long Zhang[6], Laila Ritsma[1,2] and Peter ten Dijke[1,2]

[1] Department of Cell and Chemical Biology, Leiden University Medical Center, Leiden 2333ZC, The Netherlands

[2] Oncode Institute, The Netherlands

[3] Department of Microbiology, Tumor and Cell Biology, Karolinska Institutet, Biomedicum Quarter 7B-C Solnavagen 9, 17165 Solna, Stockholm, Sweden

[4] Bioinformatics Institute (A*STAR), 30 Biopolis street, 07-01 Matrix, Singapore 138671

[5] Cancer Science Institute of Singapore, National University of Singapore, Singapore 117599

[6] Life Sciences Institute, Zhejiang University, Hangzhou, Zhejiang 310058, China

[7] Institutes of Biology and Medical Science, Soochow University, Suzhou 215123, China

[8] Sequencing Analysis Support Core, Department of Biomedical Data Sciences, Leiden University Medical Center, 2333 ZC, Leiden, The Netherlands

[9] Department of Biological sciences, National University of Singapore, 14 Science Drive 4, Singapore 117543

[10] School of Biological sciences, Nanyang Technological University, 50 Nanyang Drive, Singapore 637551

Published in Molecular Cancer Research. 2022 Oct 4;20(10):1516-1531. doi: 10.1158/1541-7786

Abstract

Bladder cancer patients often have a poor prognosis due to the highly invasive and metastatic characteristics of bladder cancer cells. Epithelial-to-mesenchymal transition (EMT) is a dynamic process that has been causally linked to invasion and metastasis of epithelial cancers such as bladder cancer. The E3 ubiquitin ligase TNF Receptor Associated Factor 4 (TRAF4) has been implicated as a tumor promoter in a wide range of cancers. We observed, however, that low TRAF4 expression was associated with poor overall survival in bladder cancer patients. Mining of publicly available data sets complemented with our own analysis of TRAF4 expression levels in bladder cancer cell lines and biopsies demonstrated that TRAF4 inversely correlated with an EMT gene signature/protein marker expression. We investigated the mechanisms by which TRAF4 expression is regulated in bladder cancer. TRAF4 expression increased upon treatment with 5-azacitidine, a DNA methylation inhibitor, suggesting that the *TRAF4* gene is epigenetically silenced. Additionally, ERK mediated TRAF4 phosphorylation resulted in lower steady-state TRAF4 protein levels caused by higher proteasomal turnover. Functionally, we found that TRAF4 expression influences EMT status in bladder cancer cells. Knockdown of TRAF4 in epithelial bladder cancer cell lines led to gain of mesenchymal genes and loss of epithelial integrity. Reciprocally, stable overexpression of TRAF4 in mesenchymal cells led to decreased migratory and invasive properties. Transcriptomic analysis of dysregulated TRAF4 expression in bladder cancer cell lines revealed that high TRAF4 expression enhanced the bone morphogenetic protein (BMP)/SMAD and inhibited the nuclear factor (NF)-κB signaling pathway. Mechanistically, we showed that TRAF4 targets the E3 ubiquitin ligase SMURF1, a negative regulator of BMP/SMAD signaling, for proteasomal degradation in bladder cancer cells. TRAF4 was found to be positively correlated with phosphoSMAD1/5, and negatively correlated with phospho-NFkb-p65 in patients. We showed that genetic and pharmacological inhibition of SMURF1 inhibited the migration of aggressive mesenchymal bladder cancer cells. Our findings could provide insights for the development of new therapeutics for bladder cancer patients with aggressive disease.

Introduction

Bladder cancer is a highly prevalent cancer with poor clinical outcomes, especially in advanced stages of progression when the cancer starts invading the bladder muscle1. Epithelial to mesenchymal transition (EMT) has been implicated in bladder cancer progression and metastasis. EMT is a dynamic process in which epithelial cells lose their cell–cell contacts and apical–basal polarity and gain mesenchymal traits with increased migration and invasion abilities2,3. Cells lose the expression of epithelial markers such as E-Cadherin and gain the expression of mesenchymal markers such as N-Cadherin4. This process is orchestrated by EMT-inducing transcription factors, including SNAIL and SLUG5,6. Transforming growth factor-β (TGF-β) signaling pathway is known to stimulate EMT7. Subsets of (mesenchymal) bladder cancer patients were found to have an overly active MAP kinase pathway; advanced and/or muscle invasive bladder cancer patients were found to have gain of function mutations in upstream activators of ERK. i.e. in fibroblast growth factor (FGF) or amplification of *RAF1* kinase[8,9]. Active ERK MAP kinase may cooperate with other signaling pathways to promote EMT of bladder and other cancer cells[10,11].

Subsets of (mesenchymal) bladder cancer patients were found to have an overly active MAP kinase pathway; advanced and/or muscle invasive bladder cancer patients were found to have gain of function mutations in upstream activators of ERK. i.e. in fibroblast growth factor (FGF) or amplification of RAF1 kinase8,9. Active ERK MAP kinase may cooperate with other signaling pathways to promote EMT of bladder and other cancer cells10,11.

Tumor necrosis factor receptor-associated factor 4 (TRAF4) encodes a ring domain containing E3 ubiquitin ligase that belongs to the TRAF protein family. Most TRAF proteins control immune and inflammation processes by mediating signaling via tumor necrosis factor receptors (TNFRs) and interleukin-1/Toll-like receptors (IL-1R/TLRs)[12]. TRAF4, however, was found to be mainly involved in embryogenesis and morphogenesis[13]. In breast cancer, TRAF4 was identified as a promoter of invasion and metastasis, and functions by targeting E3 HECT-domain containing ubiquitin ligase SMURF2 for proteasomal degradation[14]TRAF4 is recruited to the active TGF-β receptor complex, where it antagonizes E3 ligase SMURF2 and facilitates the recruitment of deubiquitinase USP15 to the TGF-β type I receptor (TβRI. SMURF2 is recruited via to TGF-β type I receptor (TβRI) to mediate TβRI polyubiquitination and proteasomal degradation. By targeting the negative regulator SMURF2, TRAF4 promoted

TGF-β signaling, EMT and metastasis in breast cancer cells[14]TRAF4 is recruited to the active TGF-β receptor complex, where it antagonizes E3 ligase SMURF2 and facilitates the recruitment of deubiquitinase USP15 to the TGF-β type I receptor (TβRI. Moreover, TRAF4 was found to be a critical factor driving breast prostate, lung, and glioma tumor progression [15–18]. The role of TRAF4 in bladder cancer has not been investigated.

Here, we report that in contrast to its role in other cancer subtypes, TRAF expression positively associated with good prognosis in bladder cancer. We uncovered how TRAF4 expression becomes compromised in aggressive bladder cancer cells and elucidated how this low TRAF4 expression influences EMT and may trigger bladder cancer progression. Moreover, using transcriptional profiling, as well as genetic and pharmacological intervention approaches, we elucidated the contribution of the NF-kb and BMP pathways that are affected upon TRAF4 dysregulation. Moreover, we confirmed these correlations using material from bladder cancer patients. Our findings may therefore be of importance for the treatment of bladder cancer patients with low TRAF4 expression.

Materials and methods

Cell culture conditions

Bladder cancer cell lines and 293T were purchased from ATCC (American Type Culture Collection). Cells were grown in Dulbecco's modified eagle medium (DMEM) supplemented with 10% fetal bovine serum and penicillin/streptomycin. Cells were regularly tested for the absence of mycoplasma contamination and were genotyped and authenticated. Cells were grown in 5% CO2 atmosphere incubator at 37˚C. Where appropriate, cells were treated with BMP6 (50ng/ml), TNF-a (10ng/ml) MG132 (2μM), LDN193189 (120nM), SMURF1i-A01 (5 or 10μM), MEK (PD0325901, 2μM), 5'-Azacytidine (5μM) and Cycloheximide (10μg/ml) for the indicated hours.

Transient transfection

293T cells were transfected with the indicated plasmids using calcium chloride and HEPES buffered saline (pH 6.95). After an overnight incubation, cells were washed twice with 1X PBS solution and replenished with fresh serum containing media. HT1376 cells were transfected using lipofectamine 2000 according to manufacturer's protocol. The following vectors and its derivates were used: pcDNA3.1 (6xMyc) TRAF4, pFLAG-CMV SMURF1, GFP-ERK1 was a gift from Rony Seger (Addgene plasmid # 14747)[43]and GFP-TRAF4 was a gift from Ying Zhang (Addgene plasmid # 58318)[37].

Stable transfection

Stable knockdown of TRAF4 in RT4, HT1376 or over-expression in T24 cells were generated using short hairpin RNAs through lentiviral transduction. 293T cells were transfected with pLKO.1 puro vectors (Sigma Mission shRNAs) or pLV-IRES Lenti Puro TRAF4 along with lentiviral packaging plasmids (pCMV-VSVG, pMDLg-RRE and pRSV-REV). The media containing viral particles were collected 48 hours later and passed through 0.45 μM filter. The supernatant with Polybrene (0.01%) was used to transduce bladder cancer cells. The cells were further selected with Puromycin (1μg/ml) containing medium. The list of short hairpins used for knockdown are provided in Sup. Table 6.

Immunofluorescence

Labelling of plasma membrane was achieved with CellMask™ Orange plasma membrane stain (ThermoFisher) solution. RT4 cells were treated with the solution according to manufacturer's instructions and images were captured soon after using Leica fluorescence microscope.

In vivo phosphorylation experiment

Transfected 293T cells were lysed in ELB buffer (250mM NaCl, 0.5%Nonidet P-40, HEPES 50mM, pH 7.3), supplemented with protease inhibitors and serine/threonine phosphatase inhibitors: 50mM sodium fluoride and 10mM b-glycerophosphate. Protein concentration was estimated on the lysates using a bicinchoninic acid protein assay Kit (5000111, Bio-Rad). Equal protein concentrations for each of the samples were incubated with Myc antibodies overnight, followed by incubation with Protein G beads for 1 hour at 4˚C. After several washing steps with 1X lysis buffer, beads were boiled in 2X sample buffer. The resulting supernatants were processed for immunoblotting.

Culturing of cell spheroids

Cell spheroids were generated using RT4 cells. 1.5% agarose was boiled until it dissolved in 1XPBS, then added onto a sterile 96-well plate (100μl each well) and it was let to solidify. About an hour later, RT4 cells were trypsinized, counted and diluted in media. About 200μl of media containing the appropriate amount of cells were added onto the agarose beds formed on the 96-well plate. The plate was spun down at 1000 RPM for 2 minutes and incubated at 37˚C CO2 incubator overnight. The following day, cell spheroids were checked

under a Leica microscope. Spheroids were assessed for circularity using ImageJ software.

Assessment of ubiquitination

Cells were washed in ice cold 1XPBS (twice) and then lysed with RIPA buffer (25mM Tris HCl, pH 7.4, 150mM NaCl, 1%Nonidet P-40, 1%SDS, 0.5%sodium deoxycholate), supplemented with protease inhibitors and 10mM N-ethylmaleimide. Lysates were sonicated, boiled at 95˚C for 5 minutes and diluted with RIPA buffer containing 0.1% SDS. Lysates were centrifuged at 4˚C for 15 minutes. Thereafter, protein estimation was performed and equal amounts of lysates were incubated with Myc antibodies overnight, followed by incubation with Protein G beads for 1 hour at 4˚C. After several washing steps with 1X lysis buffer, beads were boiled in 2Xsample buffer. The resulting supernatant was processed for immuno-blotting.

Transcriptomics, gene signatures, pathway analysis and enrichment scores

TRAF4 was knocked down using shRNA in HT1376 using lentiviral transduction. Cells with empty vector (pLKO) was used as control. Four independent experimental replicates were used for each condition. T24 cells stably over-expressing Myc-TRAF4 or empty vector (Myc-tag) were generated. Again, four independent experimental replicates were used. The cells were processed for RNA extraction and sent to BGI Tech (Hong Kong) for further processing. RNA-Seq files were processed using the opensource BIOWDL RNAseq pipeline version 3.0.0 (https://zenodo.org/record/3713261#.X4GpD2MzYck) developed at the LUMC. The pipeline performs FASTQ pre-processing (including quality control, quality trimming, and adapter clipping), RNA-seq alignment, read quantification, and optionally transcript assembly. FastQC was used for checking raw read QC. Adapter clipping was performed using Cutadapt (v2.8) with default settings. RNA-Seq reads' alignment was performed using STAR (v2.7.3a) on GRCh38 reference genome. The gene read quantification was performed using HTSeq-count (v0.11.2). The gene annotation used for quantification was Ensembl version 99. Using the gene read count matrix, CPM was calculated per sample on all annotated genes. EdgeR (v3.28.1) with TMM normalization was used to perform differential gene expression analysis. Benjamini and Hochberg FDR was computed to adjust p values obtained for differentially expressed genes. For pathway analysis, gene signatures were obtained from previous studies[44,45](Sup. Table 4). Thereafter, changes in gene expression were compared with gene signatures and enrichment scores were obtained (Sup. Table 5). The enrichment scores of gene signatures were estimated using R GSVA v1.36.2[46].

Quantitative real-time PCR

Total RNA from cells was isolated using the NucleoSpin RNA II kit (740955, BIOKE) using the manufacturer's instructions. Thereafter, 1µg of RNA from each sample was used to perform cDNA synthesis using the RevertAid First Strand cDNA synthesis kit (K1621, Thermo Fisher Scientific). Real time PCR was performed with GoTaq qPCR Master Mix (A6001, Promega) using CFX Connect Detection System (1855201, Bio-Rad). GAPDH was used as internal control for normalization. Experiments are performed as technical triplicates. A list of primers that were used are provided in Sup. Table 6.

MTS cell viability/proliferation assay

To measure the proliferative capacities, cells were seeded on 96-well plates with 100µl of media. The following and subsequent days, 20µl of MTS solution was added per well and incubated in CO2 incubator for 1.5 hours. Thereafter, absorbance was measured on a luminometer at 490nm.

Luciferase reporter assay

Luciferase reporter assays were performed using Dual luciferase reporter system (Promega). BRE-luciferase or NF-kb reporter plasmid was transfected with either control empty vector or TRAF4 and CMV-Renilla in 293T cells seeded on a 24-well plate. About 72 hours post-transfection, cells were stimulated overnight with BMP6 (50ng/ml) or TNF-a (10ng/ml) in serum free media. The following day, cells were lysed in Passive lysis buffer (Promega) and relative luciferase units and renilla values were measured using a Luminometer.

Transwell invasion assays

HT1376, T24 or MBT-2 cells were grown in 10 cm dishes and serum starved overnight. The following day, cells were trypsinized and resuspended in 0.5% serum containing media; about 50,000 were seeded onto the upper chambers. The lower chambers (wells) were filled with 2% serum containing media and incubated overnight. The following day, cells were fixed in ice-cold methanol for 10 minutes and stained with crystal violet solution. The inner side of the chambers were wiped clean using cotton swabs dipped in 1XPBS to remove remaining cells. Migrated cells were visualized through brightfield microscope and images were captured at four random sites and quantified.

Site directed mutagenesis

PCR reactions were performed using Quik-Change XL kit by Agilent Technologies (catalogue no.200517-4) according to manufacturer's instructions. The presence of mutants was confirmed by sequencing. The list of primers that were used is provided in Sup. Table 6.

Immunoblotting

Cells were lysed in RIPA buffer (150mM NaCl, 1% Nonidet P-40, 0.5% sodium deoxycholate, 0.1% sodium dodecyl sulfate, 50mM Tris pH 8.0), supplemented with protease inhibitors and phosphatase inhibitors, 50mM sodium fluoride, 100mM b-glycerophosphate and 1mM sodium orthovanadate. Protein estimation was performed on the lysates and equal amounts of protein lysates were boiled in 2X sample buffer. Thereafter, samples were loaded onto 10% SDS-PAGE gels and transferred onto 0.45µM PVDF membranes (Millipore). The membranes were blocked in 5% milk and probed with specific antibodies overnight at 4˚C. For visualization of protein signals, blots were incubated with secondary antibodies which were HRP-linked and detected using chemiluminescence. The following antibodies were used: TRAF4 1:2000 (D1N3A, CST), E-cadherin 1:1000 (Cat no. 610181, BD), N-cadherin 1:1000 (Cat no. 610920, BD), Vimentin 1:5000 (CST), SLUG 1:1000 (C19G7, CST), SNAIL 1:1000 (C15D3, CST), Flag 1:5000 (M2, Sigma Aldrich), phospho-Serine 1:1000 (612546, BD), SMURF1 1:1000 (45-K, Santa Cruz), Myc 1:5000 (9E10, Santa Cruz), HA 1:5000 (Y11, Santa Cruz), GFP 1:5000 (FL, Santa Cruz) and GAPDH 1:10,000 (MAB374, Millipore).

Wound-healing assays on Incucyte®

T24 cells were trypsinized and counted, then about 25,000 cells were seeded on each well of a 96-well plate (Essen ImageLock™) and let to attach in the CO2 incubator for 5 hours. Thereafter, media containing serum was removed and replaced with serum free media and cultured overnight. The following day, a woundmaker tool (4563, Essen) was used to produce wounds on the 96-well plate. After washing 2 times with 1XPBS, cells were replenished with 100µl of 0.5% serum containing media with the indicated treatments. The plate was then placed into the Incucyte® Systems for Live-Cell Imaging and Analysis. Real-time images of (migrating) cells were captured every 1 hour and wound closure was analysed. About 10-12 well replicates were used for each condition to produce statistical error and significance.

Immunohistochemical staining

Tissue microarrays containing bladder cancer samples of Stages 1, 2 and 3, as well as adjacent normal tissue and healthy bladder tissue were purchased from Biomax (BL802b, Biomax, U.S. Sections were deparaffinized and rehydrated, followed by heat induced antigen retrieval for 20 minutes. For the Nfκb p65 and phospho-SMAD1/5/8 antibodies, antigen retrieval was performed in 0.01 mol/L sodium citrate/0.05% Tween (pH6). For the TRAF4 antibody, this was performed in 10 mmol/L TRIS /1 mmol/L EDTA /0.05% Tween (pH9) Sections were blocked for 30 minutes with 1%BSA and 0.1%Tween, followed by overnight incubation with primary antibodies at 4˚C. Primary antibodies used were TRAF4 (1:50, HPA052377, Atlas, Bromma Sweden), NFkB-p65 (phospho-Ser311) (1:100, #11260, Signalway antibody, Uithoorn, the Netherlands) and phospho-SMAD1/5/8 (1:50, #9511, Cell Signaling, Leiden, The Netherlands). Sections were incubated with secondary antibody Alexa Fluor 488 donkey anti-rabbit (1:250, A-21206, Invitrogen, Landsmeer, the Netherlands) for 2 hours at room temperature, followed by 10 minutes of DAPI staining. Slides were digitalized using Pannoramic 250 flash III slide scanner (3DHISTECH, Budapest, Hungary) and staining for all antibodies were scored by two independent observers and their average scores were considered. TRAF4, NFkB-p65 (phospho-Ser311), and phospho-SMAD1/5/8s staining were scored combining the staining intensity (0: no staining, 1: low staining, 2: medium staining, 3: high staining) and percentage of positive tumour cells (TRAF4) or percentage of tumour cells with nuclear staining (NFkB-p65 (phospho-Ser311) and phospho-SMAD1/5/8 (0: 0%, 1: 1-5%, 2: 6-25%, 3: 26-50%, 4: 51-75%, 5: 76-100%). Staining from normal bladder tissue samples (n=8) were not considered for analysis for pSMAD1/5/8 and p-p65 samples. Representative photos of TRAF4 staining on grade 1, 2 and 3, as well as low and high NF-kb -phospho-p65 and phospho-SMAD1/5/8 staining were generated using the Caseviewer software version 2.0 (3DHISTECH, Budapest, Hungary).

Statistics analyses

Bar graphs show mean standard deviation (SD) or mean standard error (SEM) as indicated in the figure legends. Student's t test, one-way ANOVA or two-way ANOVA, as indicated in the figure legends, were used for the analysis of significance and p value. Kaplan-Meier graph was plotted using survival curve (GraphPad prism). For regression plots, Pearson's r was used to analyse correlation. All tests were two-tailed.

Results

TRAF4 expression negatively correlates with bladder cancer progression

We investigated the correlation between *TRAF4* mRNA expression and overall survival in bladder cancer patients across all stages. Kaplan–Meier analysis of publicly available data from The Cancer Genome Atlas Urothelial Bladder Carcinoma (TCGA BLCA) dataset, which was obtained from the Human Protein Atlas www.proteinatlas.org, revealed that bladder cancer patients with a lower level of *TRAF4* expression had a significantly lower survival probability than those with a higher *TRAF4* expression level (Figure 1A). To further confirm these observations, we performed immunohistochemical analysis of TRAF4 protein expression using tissue microarray samples obtained from Biomax U.S. (BL802b). Our data revealed significant differences in TRAF4 protein expression between stage 1 and stage 2/3 tumor samples, but the expression differences between stage 1 and adjacent normal tissue or normal bladder tissue samples were nonsignificant (Figure 1B and 1C). To further corroborate our initial observations, we cross-checked *TRAF4* expression in a recently compiled meta-cohort study of 2411 sets of bladder tumor data[19]. The classification comprised six distinct molecular subtypes: Her2L (Her2-like), Pap (papillary), Neu (neural), Lum (luminal), SCC (squamous cell carcinoma) and Mes (mesenchymal). We observed that *TRAF4* expression was lowest in the SCC and Mes subtypes, which had the poorest survival outcomes (Figure 1D). EMT scoring can be performed using a specific EMT gene signature[20]. It is noteworthy that the SCC and Mes subtypes had the highest EMT scores, meaning that cells of these tumors are most likely to be mesenchymal-like in phenotype[19]. Furthermore, we extended our EMT scoring to bladder cancer cell lines. Using publicly available data obtained in 59 (human) bladder cancer cell lines[21], we calculated the EMT scores (Figure 1E, Sup. Table 1). We defined cell lines with a negative EMT score as more epithelial-like and cell lines with a positive EMT score as more mesenchymal-like. Consistent with the results obtained in patient biopsies, significant negative correlations were found between *TRAF4* expression and the EMT score in these 59 bladder cancer cell lines (Figure 1F). We selected 5 bladder cancer cell lines, i.e. RT4 and HT1376, with negative EMT scores, and T24, J82 and UMUC3, with positive EMT scores, for further consideration in our study. We next examined whether TRAF4 expression correlates with the 'EMT status' of these cell lines at the protein level by Western blot analysis. As shown in Figure 1G, TRAF4 expression was higher in epithelial cell lines expressing higher levels of E-cadherin and lower levels of the mesenchymal markers N-cadherin and Vimentin[5]. In contrast, TRAF4 expression was lower in mesenchymal cell lines with lower E-cadherin levels but higher N-cadherin and Vimentin levels. Importantly, the epithelial cell lines also had higher *TRAF4* mRNA expression levels than the mesenchymal cell lines (Figure 1H). Collectively, our results indicate that TRAF4 expression is higher in less aggressive epithelial bladder cancer cells than in more aggressive mesenchymal bladder cancer cells.

TRAF4 is epigenetically repressed and is phosphorylated at serine 334 by ERK

We then sought to determine the reasons for the low expression of *TRAF4* in mesenchymal cells. We subjected three mesenchymal cell lines to 5-azacitidine (5-AZA, a compound that blocks DNA methylation) treatment for one week. As shown in Figure 2A, *TRAF4* expression was rescued upon treatment in these cell lines, suggesting that *TRAF4* is epigenetically repressed. As a control, we measured the expression of *CDH1* (encoding E-cadherin), which is known to be epigenetically repressed in many mesenchymal cancer cells; its expression was increased upon 5-AZA treatment (Figure 2B). Surprisingly, however, the treated cells did not show consistent upregulation of TRAF4 protein expression, although E-cadherin expression was upregulated in 2 of the 3 cell lines (Sup. Figure 1A). This suggested the existence of additional mechanisms that control TRAF4 protein levels. We performed a cycloheximide pulse–chase experiment to analyze the protein stability of TRAF4 in different cell lines. The TRAF4 protein was less stable in UMUC3 cells than in RT4 and HT1376 cells (Figure 1C). To determine the existence of specific posttranslational modifications that regulate TRAF4 protein stability, we performed mass spectrometry analysis after overexpression of Flag-TRAF4 in 293T cells (Sup. Table 2, Sup. Figure 2A). We observed that TRAF4 undergoes several phosphorylation events at serine and threonine residues scattered through its length (Figure 2D, Sup. Figure 2A).

To determine whether phosphorylation at these sites affects the TRAF4 expression level, we performed site-directed mutagenesis to mutate the candidate serine/threonine residues to glutamic acid (E) residues in order to mimic phosphorylation, or alanine (A) residues in order to block phosphorylation. We ectopically expressed these TRAF4 mutants in 293T cells and assessed their expression levels. As shown in Figure 2E and 2F, compared to modifications at the other sites, mutation of serine 334 to glutamic acid significantly reduced the TRAF4 expression level, and reciprocally, mutation of serine 334 to alanine increased its expression level.

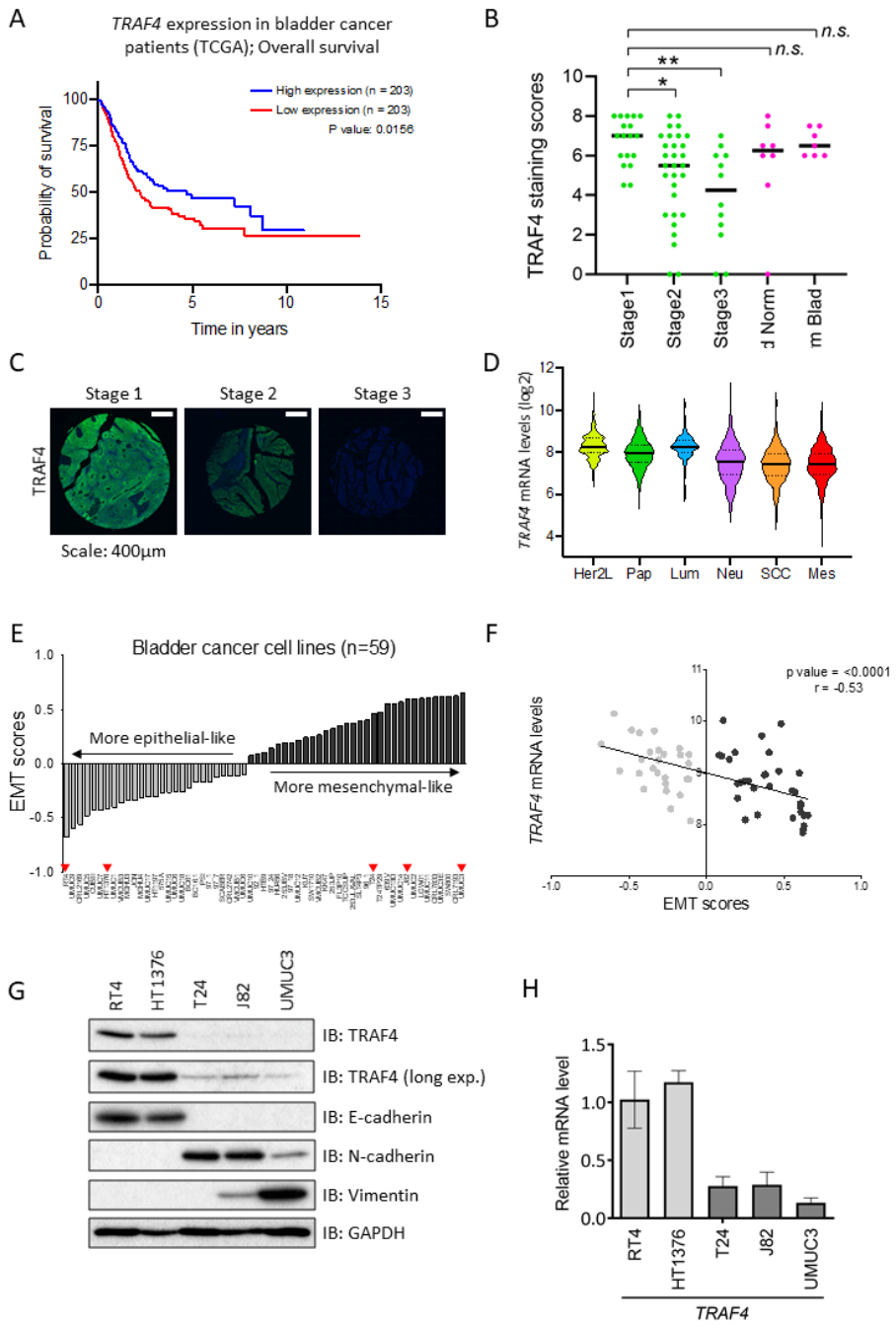

< Figure 1. TRAF4 is downregulated in aggressive bladder tumors and mesenchymal bladder cancer cell lines

(A) Kaplan–Meier plot showing the overall survival of bladder cancer patients stratified by TRAF4 expression. Data were obtained and reproduced from TCGA (obtained from Human Protein Atlas), and the median Fragments Per Kilobase of transcript per Million mapped reads (FKPM) value was taken as the TRAF4 expression cutoff. **(B)** Graph showing TRAF4 expression through scores obtained from immunohistochemical analysis of a tissue microarray; *P ≤ 0.05 and **P ≤ 0.01 calculated using one-way ANOVA; n.s. indicates a nonsignificant P value. **(C)** Representative immunohistochemical images of TRAF4 expression (green) in the tissue microarray from stage 1-3 bladder tumors are shown. Scale bar, 400 mm. **(D)** Violin plot showing the TRAF4 expression level (and distribution) in different subtypes of bladder cancer; Her2L: Her2-like (n=253), Pap: papillary (n=674), Lum: luminal (n=107), Neu: neural (n=448), SCC: squamous cell carcinoma (n=333) and Mes: mesenchymal (n=308). The black bars in the middle of the distribution indicate the medians. The subtypes are arranged according to their EMT scores19,20. **(E)** Plot showing the EMT scores in 59 bladder cancer cell lines; the light grey bars indicate cell lines with a negative EMT score, the dark grey bars indicate cell lines with a positive EMT score, and the red arrowheads indicate the cell lines that were used for further investigation21. **(F)** Regression plot of TRAF4 expression levels vs. EMT scores in 59 bladder cancer cell lines. **(G)** Immunoblot analysis showing the expression of TRAF4 and other EMT marker proteins. GAPDH, loading control. **(H)** Real-time PCR data showing TRAF4 mRNA expression in cell lines. The error bars indicate ± SD. Epithelial cell lines (light grey bars) had significantly higher TRAF4 expression than mesenchymal cell lines (dark grey bars).

Serine 334 in TRAF4 appears to be highly conserved in the other species examined (Sup. Figure 1B). Ectopic expression of Myc-TRAF4 mutants in UMUC3 cells confirmed the results obtained in 293T cells (Figure 2G). A cycloheximide pulse chase assay revealed that the S334E mutant was indeed less stable than WT TRAF4 or the S334A mutant (Sup. Figure 1C and 1D). Moreover, addition of the proteasome inhibitor MG132 rescued the low expression level of the S334E mutant, suggesting that its low expression is due to proteasomal-mediated degradation (Sup. Figure 1E). A phosphorylation prediction tool (Human Protein Reference Database, PhosphoMotif Finder) revealed that serine 334 could be a putative extracellular-signal-regulated kinase (ERK) mitogen-activated protein (MAP) kinase phosphorylation site. When we overexpressed ERK1 along with TRAF4 in 293T cells, the TRAF4 expression level was significantly reduced (Sup. Figure 1F). Importantly, ERK1 was not able to influence the expression level of the S334A mutant (Sup. Figure 1F). MG132 was also able to rescue the ERK1-mediated decrease in the expression of TRAF4, suggesting that ERK1-mediated phosphorylation of TRAF4 induces its proteasomal degradation (Sup. Figure 1G). To determine whether ERK1 can induce the phosphorylation of TRAF4 and whether this effect can be enhanced by MG132, we assessed the levels of TRAF4 pSerine upon ERK1 expression. As shown in Figure 2H, co-transfection of ERK1 with TRAF4 indeed increased TRAF4 phosphorylation, and this effect was further enhanced upon treatment with MG132.

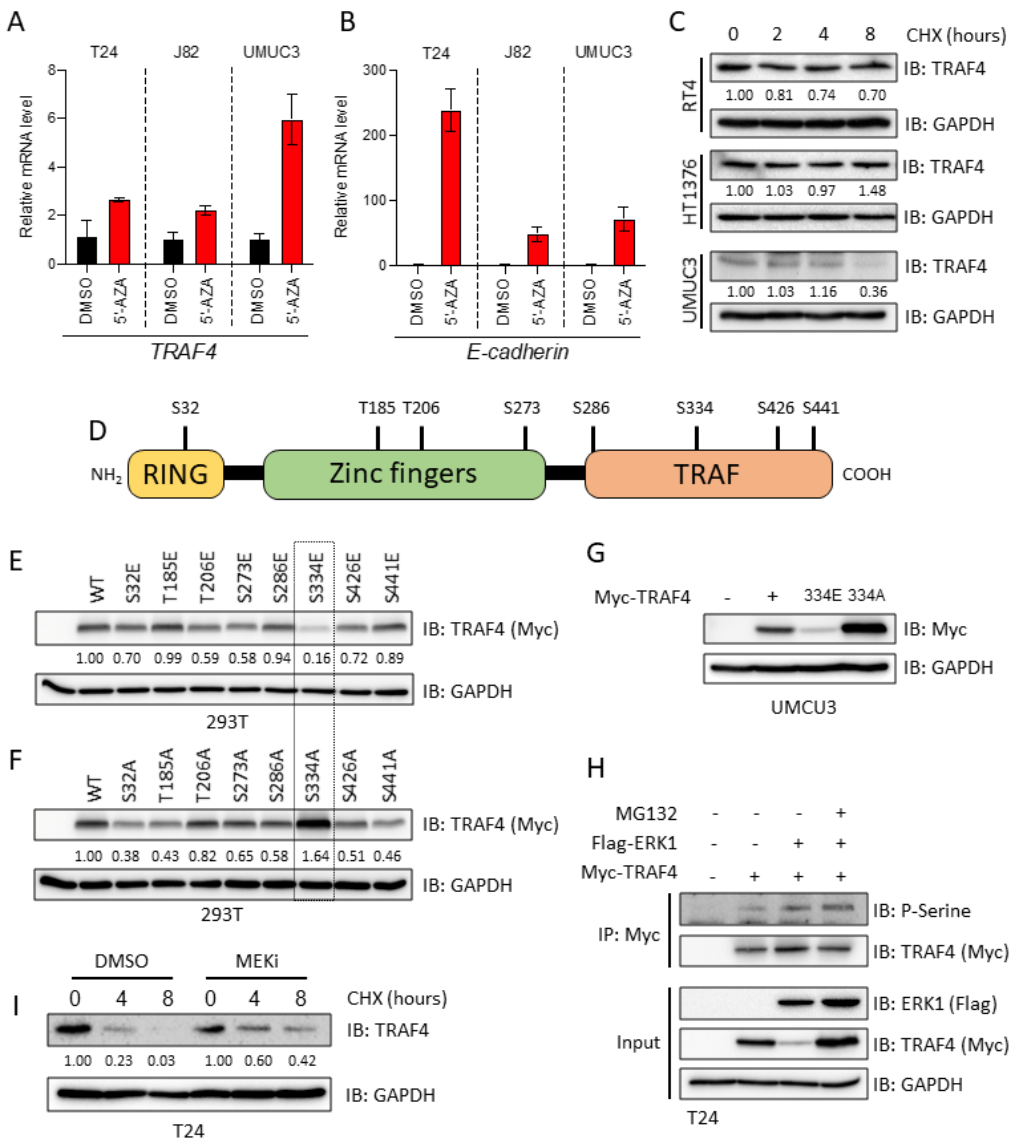

< Figure 2 .TRAF4 is repressed in mesenchymal (bladder cancer) cell lines at the epigenetic and proteomic levels

(A) Real-time PCR results showing changes in the TRAF4 mRNA level in mesenchymal cell lines after treatment with 5-azacitidine (5-AZA). **(B)** Real-time PCR results showing changes in the CDH1 mRNA level in cell lines after treatment with 5-AZA; the error bars indicate ± SD. **(C)** Immunoblot results showing the endogenous TRAF4 levels in the indicated cell lines after treatment with cycloheximide (CHX). GAPDH, loading control. The numbers indicate the relative quantitative TRAF4 levels with respect to the loading control GAPDH. **(D)** Schematic representation of TRAF4 showing the distinct domain structures and the candidate phosphorylated serine and threonine residues that were identified using mass spectrometric analysis. **(E)** Immunoblot results from 293T cells transfected with expression constructs for either TRAF4 or the TRAF4 glutamic acid **(E)** mutant. GAPDH, loading control. The numbers indicate the relative quantitative TRAF4 levels with respect to the loading control GAPDH. **(F)** Immunoblot results from 293T cells transfected with expression constructs for either TRAF4 or the TRAF4 alanine **(A)** mutant. GAPDH, loading control. The numbers indicate the relative quantitative TRAF4 levels with respect to the loading control GAPDH. **(G)** Western blot analysis of ectopic Myc-TRAF4 WT and the S334E and S334A mutants in the UMUC3 cell line. GAPDH, loading control. **(I)** Western blot analysis of TRAF4 expression in T24 cells treated with CHX at the indicated times, in the presence of DMSO (control) or MEKi. GAPDH, loading control. The numbers indicate the relative quantitative TRAF4 levels for both DMSO and MEKi (PD0325901) treatment separately, with respect to the loading control GAPDH.

Moreover a selective small molecule MEK (an upstream kinase of ERK) inhibitor (MEKi, PD0325901) prolonged TRAF4 stability T24 cells overexpressing TRAF4 (Figure 2I) and slightly enhanced steady-state TRAF4 level in 293T cells expressing Myc-TRAF4 (Sup. Figure 1H). This observation was consistent in the UMUC3 and T24 cell lines, where the endogenous TRAF4 level was slightly increased by MEKi treatment, while *TRAF4* mRNA level remained relatively unaffected (Sup. Figure 1I, 1J, 1K and 1L). Taken together, our results suggest that phosphorylation of TRAF4 at serine 334 by ERK leads to a decrease in its expression via proteasome-mediated degradation.

Knockdown of TRAF4 in epithelial cell lines leads to loss of epithelial integrity and gain of mesenchymal markers

Since we observed that TRAF4 expression is reduced in mesenchymal cells compared to epithelial bladder cancer cells, we next investigated the consequences of TRAF4 knockdown in the epithelial cancer cell lines RT4 and HT1376. Depletion of TRAF4 in RT4 cells using the two independent short hairpin RNAs (#4 and #5) with the highest knockdown efficiency (Sup. Figure 3A) led to increases in the mRNA expression levels of the mesenchymal markers *CDH2* (encoding N-cadherin) and *SNAI2* (encoding SLUG) (Figure 3A). SLUG is a well-studied EMT transcription factor that has been described to play roles in cadherin switching and malignancy in bladder cancer progression[22]. Notably, another major EMT-inducing transcription factor, *SNAI1* (encoding SNAIL), was consistently downregulated upon TRAF4 knockdown.

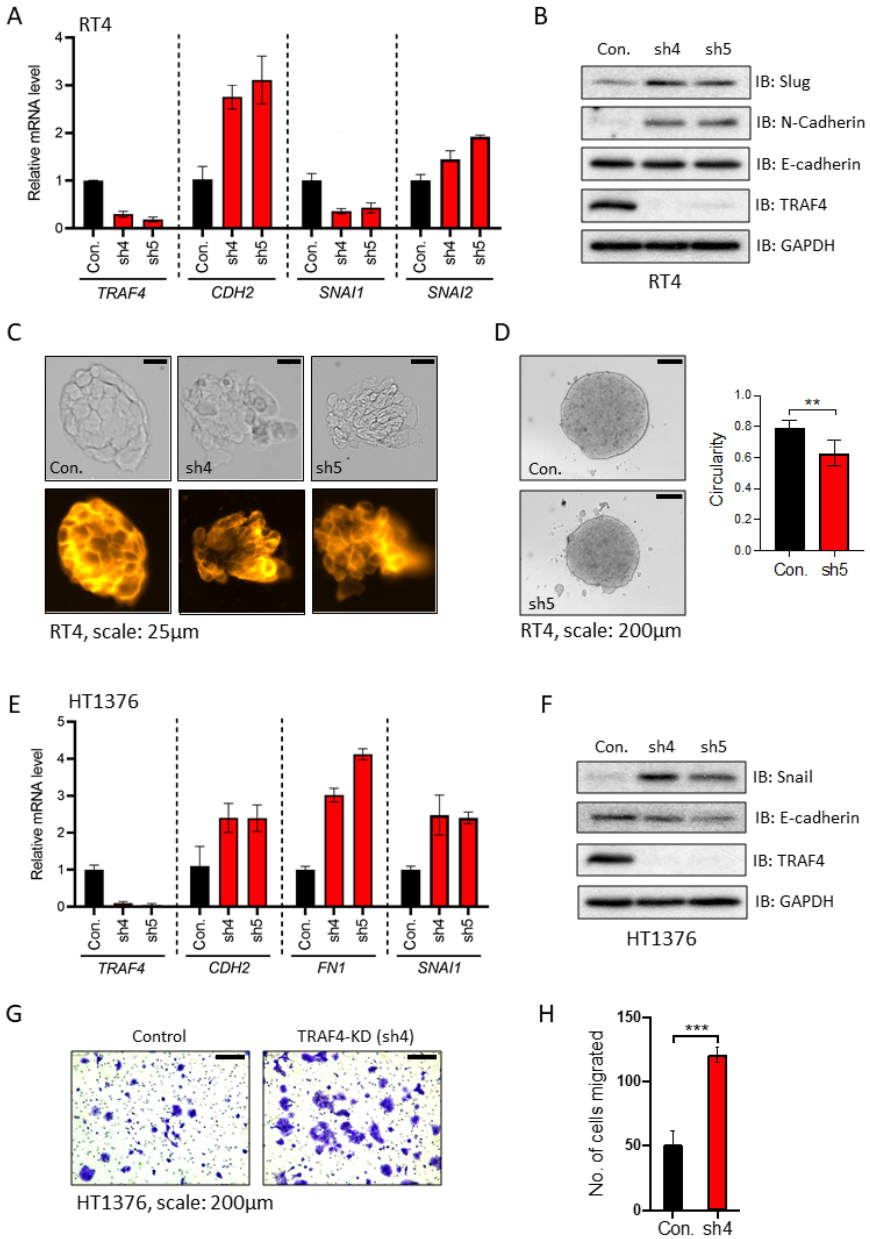

< Figure 3.Knockdown of TRAF4 in epithelial (bladder cancer) cell lines leads to loss of epithelial integrity and changes in EMT marker expression

(A) Real-time PCR results from RT4 cells showing the mRNA expression levels of the indicated genes; the error bars indicate ± SD. **(B)** Immunoblot results showing changes in EMT marker protein expression in RT4 cells upon TRAF4 knockdown. GAPDH, loading control. **(C)** RT4 cell colonies visualized by brightfield imaging (top panels) or after staining with CellMask™ Orange plasma membrane stain (bottom panels); scale bar: 25 μm. **(D)** Images showing RT4 spheroids formed from control (empty pLKO vector) and TRAF4 knockdown (sh5) cells; scale bar: 200 μm. The graph shows circularities calculated from five independent spheroids of different sizes. The error bars indicate ± SD; **P ≤ 0.01 calculated using two-tailed Student's t test. **(E)** Real-time PCR results from HT1376 cells showing the mRNA expression levels of the indicated genes; the error bars indicate ± SD. **(F)** Immunoblot results showing EMT marker protein expression levels in HT1376 cells with or without TRAF4 knockdown. GAPDH, loading control. **(G)** Representative images of Transwell assays performed on HT1376 cells are shown. Cells were stained with crystal violet; scale bar: 200 μm. **(H)** Quantification of the number of migrated cells in four random fields; the error bars indicate ± SD; ***P ≤ 0.001 calculated using two-tailed Student's t test.

The increases in SLUG and N-cadherin (but not E-cadherin) expression were also observed at the protein level (Figure 3B). Besides changes in gene expression of EMT markers, we observed phenotypic changes in the integrity and architecture of cell colonies upon TRAF4 knockdown (Figure 3C). Staining with a membrane dye revealed that the borders of cells within RT4 cell colonies became disordered and that loosely attached cells appeared upon TRAF4 knockdown. The membrane staining of colonies formed by control (pLKO vector) cells resembled that of colonies formed by wild-type RT4 cells (Sup. Figure3B).

To examine whether TRAF4 knockdown affects the 3-dimensional structural architecture of cells, RT4 cell spheroids were generated. Spheroids recapitulate tumor cell clusters and can be considered, in many ways, a model more representative of *in vivo* conditions than 2-dimensional-cultured cells. Figure 3D shows spheroids formed from control RT4 (empty pLKO vector) and TRAF4 knockdown cells. We found that upon TRAF4 knockdown, several clumps of cells within the spheroids were dissociated or excluded from the main bodies. Moreover, the spheroids in the knockdown group were more irregular in shape compared to those in the control group, as determined by measurement of their circularity (Figure 3D). This cell exclusion phenotype has been observed in previous studies and is reflective of the loss of certain tight junction components in epithelial cells [23,24]. We further demonstrated the effects of TRAF4 knockdown using the epithelial cell line, HT1376. TRAF4 knockdown using 2 different shRNAs (Sup. Figure 3C) led to a significant increase in the mRNA expression levels of the mesenchymal markers *FN1* (encoding Fibronectin) and *SNAI1* (Figure 3E), and an increasing trend of *CDH2*, encoding N-cadherin. Although we saw a concomitant increase in the

level of the EMT-inducing transcription factor SNAIL (Figure 3F), we could not observe whether the N-cadherin level changed as it remained below the limit of detection. Moreover, the E-cadherin level remained at best unchanged upon TRAF4 knockdown in these cells. We hypothesized that since EMT has been linked to migratory and invasive properties, knockdown of TRAF4 would lead to enhanced invasive behavior. Knockdown of TRAF4 indeed increased the number of invaded cells, as determined by transwell assays (Figure 3G and 3H). Thus, TRAF4 knockdown in epithelial cells disrupts their epithelial architecture and organization. Importantly, TRAF4 knockdown leads to an increase in gene expression of EMT markers, disruption in epithelial architecture and organization, and importantly, an increase in their invasive capacities. This suggests that upon knockdown of TRAF4, epithelial bladder cancer cells become more mesenchymal.

Stable overexpression of TRAF4 diminishes the migratory and invasive properties of mesenchymal cells

We next assessed whether ectopic expression of TRAF4 in mesenchymal cell lines affects their functional properties. To this end, we stably overexpressed empty vector (myc-tag), TRAF4 or the TRAF4 (C/A) mutant, as shown in Figure 4A. Ectopic expression of TRAF4 slightly but significantly decreased T24 cell invasion (Figure 4B and 4C) and migration (Figure 4D and 4E) in a catalytically dependent manner, while migration was slightly increased upon ectopic expression of TRAF4. (Figure 4F). Next, we used the highly invasive mouse cell line MBT-2, which has a low TRAF4 level (Sup Figure 4A). Stable overexpression of TRAF4 in MBT-2 cells (Figure 4G) decreased their invasive ability (Figure 4H and 4I). Upon closer examination, morphologically, TRAF4-overexpressing cells tended to cluster more closely together than their control cells, especially when seeded at a low density (Sup. Figure 4B). Collectively, these findings demonstrate that TRAF4 overexpression diminishes some of the aggressive characteristics of mesenchymal cell lines.

TRAF4 targets SMURF1 for polyubiquitination and degradation

Previously, TRAF4 was shown to interact with the E3 ligase SMURF1, a negative regulator of BMP/SMAD signaling and positive regulator of EMT progression[14,25,26].We hypothesized that TRAF4 targets SMURF1 for proteasomal degradation and that this event may explain the inhibitory effect of TRAF4 on EMT in bladder cancer cells. We found that TRAF4 interacts with SMURF1 in HT1376 bladder cancer cells (Figure 5A)[27]. Consistent with the hypothesis that TRAF4 targets SMURF1 for degradation, we observed that in RT4 cells,

the SMURF1 level was decreased by overexpression of wild-type (WT) TRAF4 but not by its catalytically inactive mutant TRAF4 (C/A) (Figure 4A). Moreover, upon TRAF4 knockdown in RT4 cells, the level of SMURF1 increased compared to that in control cells (Figure 5B). This pattern was also observed in HT1376 cells (Figure 5C). The *SMURF1* mRNA level did not change upon TRAF4 knockdown in either of these cell lines (Figure 5D). Next, we tested whether TRAF4 can induce SMURF1 polyubiquitination and decrease its expression level. Co-expression of TRAF4, but not the inactive TRAF4 (C/A) mutant or the RING deletion mutant, increased the polyubiquitination (Figure 5E) and decreased the steady-state level of SMURF1 (Figure 5F).

The role of SMURF1 in promoting cancer cell invasion is well documented[26]. To examine whether SMURF1 plays a similar role in mesenchymal bladder cancer cells, we utilized the MBT-2 cell line, which expresses Smurf1 (Sup Figure 4A, B). We observed that upon SMURF1 knockdown (using two independent shRNAs, Sup. Fig 4C, D), the invasion of MBT-1 cells was significantly decreased (Figure 5G and 5H). These results were confirmed in T24 cells using a commercially available SMURF1 inhibitor, A01[28]. Of note, this SMURF1 inhibitor does not target E3 ligase activity but targets the ability of SMURF1 to bind to BMP pathway effector protein SMAD1 and SMAD5 and subsequently induce their proteasomal degradation[29]. Treatment of T24 cells with A01 significantly reduced the wound healing ability compared to those in control (DMSO-treated) cells (Figure 5I, J), while having a slightly enhanced effect on proliferation. (Figure 5K). Taken together, our results demonstrate that TRAF4 can reduce the SMURF1 protein level in bladder cancer cells and that SMURF1 enhances the migration and invasion of these mesenchymal bladder cancer cells.

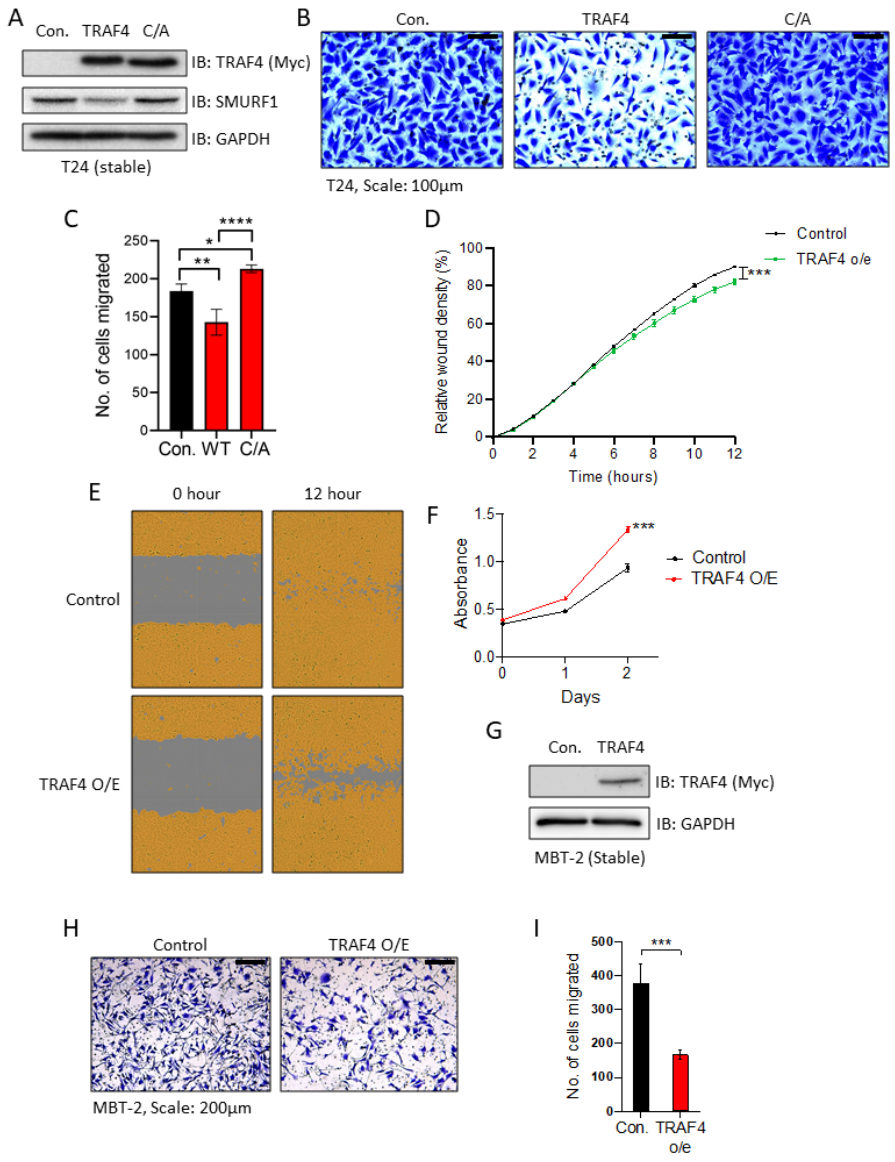

< Figure 4 .Ectopic expression of TRAF4 in mesenchymal cells inhibits their migration and invasion **(A)** Immunoblot showing T24 cells stably expressing either control vector (myc-tag), TRAF4 or the catalytically inactive TRAF4 mutant (C/A: cysteine substituted with alanine at residue C18). GAPDH, loading control. **(B)** Representative images of Transwell assays performed on T24 cells stably expressing TRAF4 or the catalytically inactive TRAF4 mutant (C/A) are shown. Cells were stained with crystal violet; scale bar: 100 µm. **(C)** Quantification of the number of migrated cells in four random fields. The error bars indicate ± SD; **P ≤ 0.01 and ****P ≤ 0.0001 calculated using one-way ANOVA. **(D)** Graph showing the relative wound widths as determined with an IncuCyte® system. Representative results from three independent experiments are shown; the error bars indicate ± SEM; ***P ≤ 0.001 calculated using two-tailed Student's t test. **(E)** Representative images related to the graph shown in D; the brown area represents the cell coverage, and the gray area indicates the initial wound produced and the remaining wound after 12 hours. **(F)** MTS cell viability/proliferation assay performed with either control T24 cells or T24 cells stably expressing TRAF4. The absorbance was measured at the indicated time points; the error bars indicate ± SD from three sample replicates; ***P ≤ 0.001 calculated using two-tailed Student's t test. **(G)** Immunoblot results for MBT-2 cells stably expressing either control vector (empty vector with a Myc-tag) or Myc-TRAF4. GAPDH, loading control. **(H)** Representative images of Transwell assays performed on control and TRAF4-overexpressing MBT-2 cells stained with crystal violet; scale bar: 200 µm. **(I)** Quantification of the number of migrated cells in four random fields. The error bars indicate ± SD; ***P ≤ 0.001 calculated using two-tailed Student's t test.

Dysregulated expression of TRAF4 in bladder cancer cell lines affects the NF-κB and BMP signaling pathways

Next, to obtain insights into the mechanisms by which TRAF4 affects bladder cancer cell behavior, we examined the effect of TRAF4-mediated dysregulation of signaling pathways. To this end, we stably overexpressed TRAF4 in T24 cells (Sup. Figure 4E), performed transcriptomic (RNA-seq) analysis and looked for changes in the gene response signatures of the eleven most commonly studied oncogenic signaling pathways. Volcano plot of T24 cells expressing empty vehicle versus TRAF4 is shown in Sup. Figure 4F. Nine of the eleven signaling pathways showed varying degrees of changes in the enrichment score. The two most prominently changes in pathways were the downregulation of the NF-κB signaling pathway and the upregulation of the BMP/SMAD signaling pathway (Figure 6A). These findings are consistent with previous reports indicating that TRAF4 can inhibit NF-kb signaling and promote BMP signaling[13,30].

We also examined the changes in gene expression upon TRAF4 depletion in HT1376 cells using two independent shRNAs. Volcano plots of HT1376 cells expressing empty vehicle versus TRAF4 sh4 and sh5 are shown in Sup. Figure 4G and H respectively. As shown in Figure 6B, 252 genes were upregulated upon TRAF4 knockdown in HT1376 cells (common to both shRNAs) and reciprocally downregulated in T24 cells upon TRAF4 overexpression (Sup. Table 3). Similarly, we detected 96 genes that were upregulated in T24 cells and downregulated in HT1376 cells compared to the corresponding control cells (Figure 6C and Sup. Table 3).

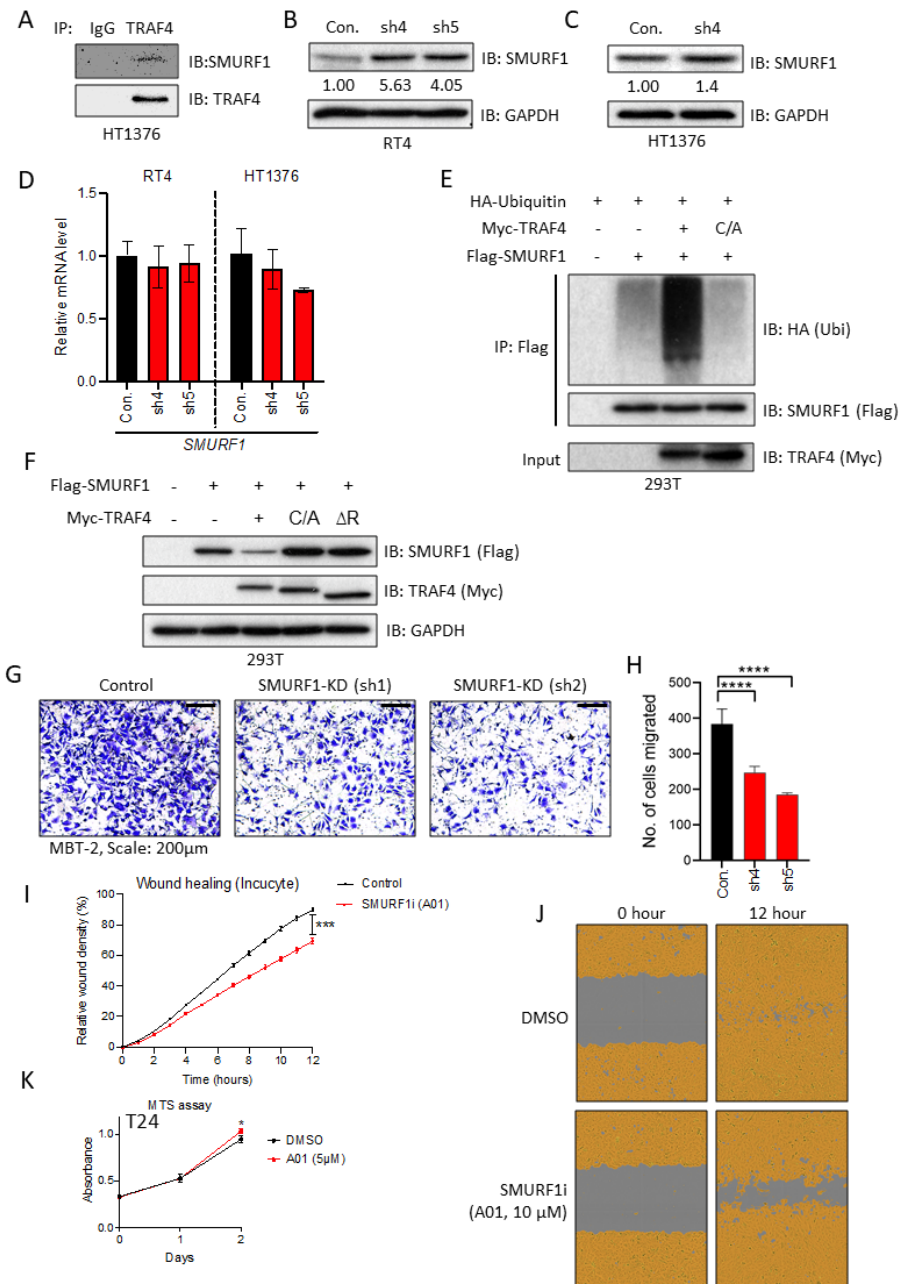

< Figure 5. TRAF4 targets SMURF1 for ubiquitination and degradation
(A) Immunoprecipitation of SMURF1 followed by western blot analysis of TRAF4 in HT1376 cells. **(B)** Immunoblot results in control (empty pLKO vector) and TRAF4 knockdown (sh4 and sh5) RT4 cells probed with the indicated antibodies. GAPDH, loading control. The numbers indicate the relative quantitative SMURF1 levels with respect to the loading control GAPDH**. (C)** Immunoblot results in control (empty pLKO vector) and TRAF4 knockdown (sh4) HT1376 cells probed with the indicated antibodies. The numbers indicate the relative quantitative SMURF1 levels with respect to the loading control GAPDH. **(D)** Real-time PCR results showing SMURF1 mRNA expression levels in RT4 and HT1376 (control and TRAF4 knockdown) cells; the error bars indicate ± SD. **(E)** A ubiquitination assay was performed with anti-Flag antibodies in 293T cells overexpressing the indicated plasmids. Cells were treated with MG132 (2 μM) overnight prior to lysis. Representative results from three independent experiments are shown. **(F)** Immunoblot results in 293T cells transfected with the indicated plasmids. GAPDH, loading control. **(G)** Representative images of Transwell assays performed on control and Smurf1 knockdown MBT-2 cells stained with crystal violet; scale bar: 200 μm. **(H)** Quantification of the number of migrated cells in four random fields. The error bars indicate ± SD; *** P ≤ 0.001 and ****P ≤ 0.0001 calculated using one-way ANOVA. **(I)** Graph showing relative wound widths as determined with an IncuCyte® system. Images were acquired every hour after wounding. T24 cells were treated with either DMSO or the SMURF1 inhibitor A01 (10 μM); the error bars indicate ± SEM; ***P ≤ 0.001 calculated using two-tailed Student's t test. Representative results from three independent experiments are shown**. (J)** Representative images related to the graph in I. The brown area represents the cell coverage, and the gray area indicates the wound initially produced and remaining after 12 hours. **(K)** An MTS assay was performed on T24 cells treated with either control (DMSO) or the SMURF1i A01 at 5 μM. The absorbance was measured at the indicated time points; the error bars indicate ± SD from three sample replicates; *P ≤ 0.05 calculated using two-tailed Student's t test.

Five BMP/SMAD target genes, i.e., *ID1*, *ID2*, *ID3*, *DKK1* and *TNFRSF11B*[31], were reciprocally regulated in the two cell lines upon TRAF4 dysregulation. These genes were downregulated upon TRAF4 knockdown in HT1376 cells and upregulated upon TRAF4 overexpression in T24 cells (Figure 6D). Upon examining the NF-κB gene signature within the set of reciprocally regulated genes, we found four common genes showing downregulation upon TRAF4 overexpression in T24 cells and upregulation upon TRAF4 knockdown in HT1376 cells (Figure 6D). We found that TRAF4 inversely correlated with the EMT status of bladder cancer cells (Figure 1F); therefore, we examined EMT gene markers within the set of reciprocally regulated genes between the two cell lines and found four genes, i.e., *FN1* (encoding Fibronectin), *TGFB2* (encoding TGF-β2), *CALD1* (encoding Caldesmon 1) and *ITGAV* (encoding Integrin subunit α-V) that are inversely linked to *TRAF4* expression (Figure 6D). Our transcriptomic analysis thus shows that dysregulated expression of TRAF4 affects NF-kb and BMP signaling pathways, as well as EMT-related genes.

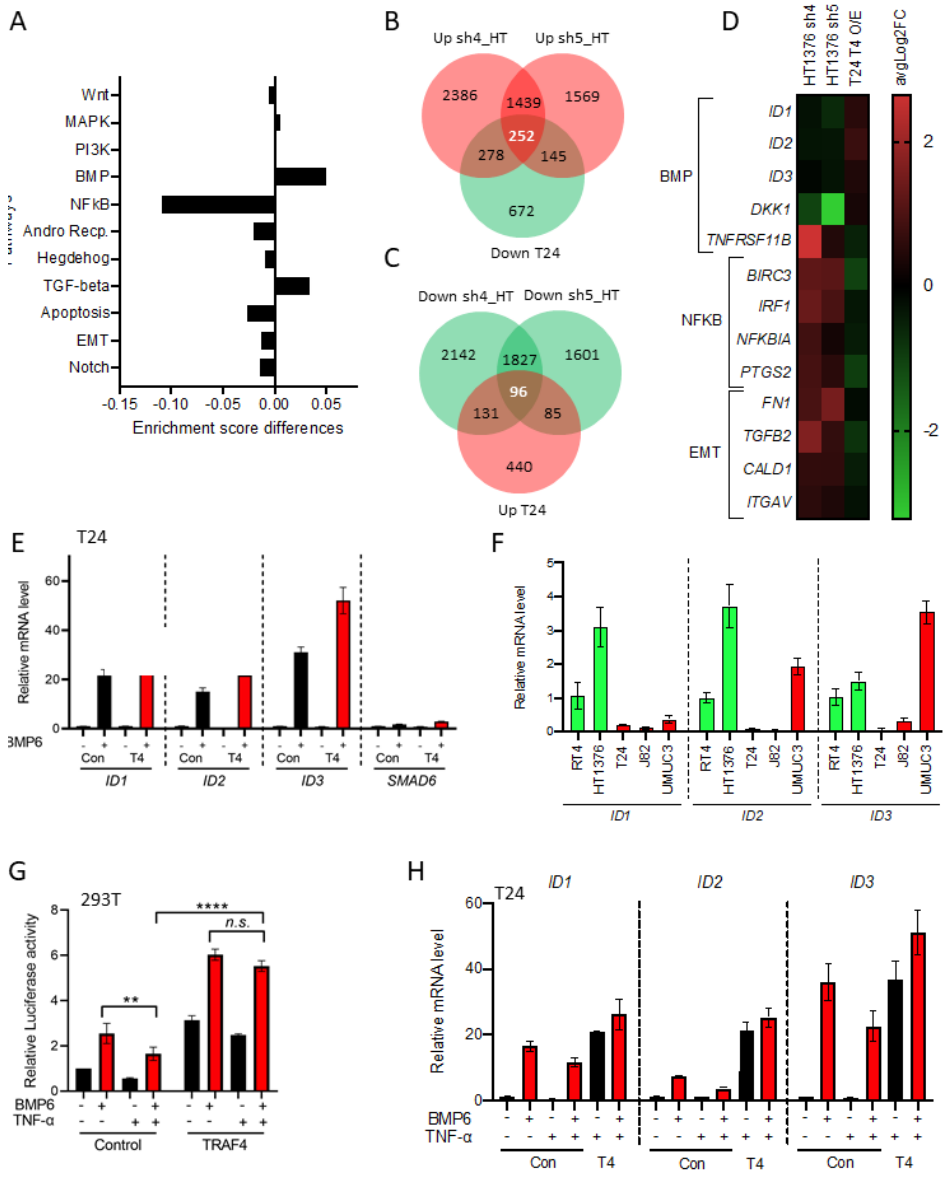

< Figure 6. Dysregulated expression of TRAF4 in bladder cancer cell lines affects BMP/SMAD- and NF-kb-responsive genes

(A) Graph showing differences in enrichment scores when TRAF4 was overexpressed in T24 cells. Gene signatures of eleven major cancer-associated signaling pathways were considered for analysis. **(B)** Venn diagram showing the numbers of genes that were upregulated in HT1376 cells transfected with two independent shRNAs targeting TRAF4 (pink) and downregulated in T24 cells with stable overexpression of TRAF4 (green) compared to the corresponding control cells. The 252 genes in the middle are the reciprocally affected common genes. The results were obtained from four independent replicates for each sample. **(C)** Venn diagram showing the numbers of genes that were downregulated in HT1376 cells transfected with two independent shRNAs targeting TRAF4 (green) and upregulated in T24 cells with stable overexpression of TRAF4 (pink) compared to the corresponding control cells. The 96 genes in the middle represent the reciprocally affected common genes. The results were obtained from four independent replicates for each sample. **(D)** Heatmap showing the common dysregulated genes in the BMP, NF-κB and EMT gene signatures in both cell lines. **(E)** Real-time PCR results showing the mRNA expression levels of the indicated genes in control (empty vector with a myc tag) vs. TRAF4-overexpressing T24 cells upon stimulation with BMP6 (50 ng/ml) for 1 hour. The error bars indicate ± SD. **(F)** Real-time PCR results showing the mRNA expression levels of ID1, ID2 and ID3 in the indicated cell lines. **(G)** A luciferase reporter assay was conducted in 293T cells transfected with the BRE-luciferase reporter, SV40 Renilla and either empty vector control or TRAF4. Transfected cells were stimulated overnight with BMP6 (50 ng/ml) and/or TNF-*α* (10 ng/ml) where indicated. The error bars indicate ± SD; **P ≤ 0.01 and ****P ≤ 0.0001 calculated using two-way ANOVA; n.s. indicates a nonsignificant P value. Representative results from three independent experiments are shown. **(H)** Real-time PCR results showing the mRNA expression levels of the indicated genes in control (empty vector with a myc tag) vs. TRAF4-overexpressing T24 cells upon stimulation with BMP6 (50 ng/ml) and/or TNF-*α* (10 ng/ml) as indicated for 1 hour. The error bars indicate ± SD.

TRAF4 promotes BMP/SMAD signaling in bladder cancer cells and antagonizes the inhibitory effect of TNFα signaling on BMP/SMAD signaling

As TRAF4 expression was positively associated with BMP signaling, we next determined the consequences of BMP stimulation on mesenchymal cells. Interestingly, we observed that canonical BMP pathway target genes (*ID1*, *ID2*, *ID3* and *SMAD6* were expressed at slightly higher levels upon BMP6 stimulation in T24 cells stably expressing TRAF4 (Figure 6E) [31,32]. This effect was also observed in MBT-2 cells (Sup. Figure 5A). Next, a BMP/SMAD response element (BRE)-luciferase transcriptional reporter assay was used to measure downstream BMP/SMAD signaling activity in 293T cells. BMP6 stimulation led to significantly higher luciferase activity in 293T cells transfected with TRAF4 than in the non-transfected control (Sup. Figure 5B). We then hypothesized that perhaps these three *ID* genes are expressed at higher levels in epithelial cell lines due to the difference in TRAF4 expression. Indeed, we observed that *ID* gene expression in the epithelial cell lines RT4 and HT1376 was generally higher than that in mesenchymal cell lines (Figure 6F). Moreover, we observed that a selective BMP type I receptor kinase inhibitor (LDN193189) rescued the inhibitory effects of TRAF4 on the wound healing ability

(Sup. Figs. 5C and 5D). Likewise, BMP6 stimulation inhibited T24 cell migration (Sup. Figs. 5E and F), while having minimal effects on proliferation Sup Figure 5G). Taken together, our results suggest that TRAF4 inhibits bladder cancer cell migration by promoting BMP/SMAD signaling.

Consistent with previous observations, overexpression of TRAF4 negatively affected NF-κB reporter activity (Sup. Figure 5H). As we observed that TRAF4 promotes BMP/SMAD signaling in bladder cancer cells, we next explored the possibility of crosstalk between BMP and NF-kb signaling and whether TRAF4 has a role therein. TNF-α stimulation inhibited BMP/SMAD signaling, as determined by measuring BRE-luc transcriptional reporter activity (Fig 6G). Interestingly, overexpression of TRAF4 mitigated the negative effect of TNF-α on BMP/SMAD signaling. Similar effects were observed when T24 cells were stimulated with a combination of BMP and TNF-α and the expression of *ID* genes was analyzed (Figure 6H). Thus, the increased NF-kb signaling associated with a low TRAF4 level in mesenchymal cells may lead to a decrease in BMP/SMAD signaling. Thus, TRAF4 can promote BMP/SMAD indirectly by antagonizing the inhibitory effect of TNFα/ NF-kb signaling on BMP/SMAD signaling.

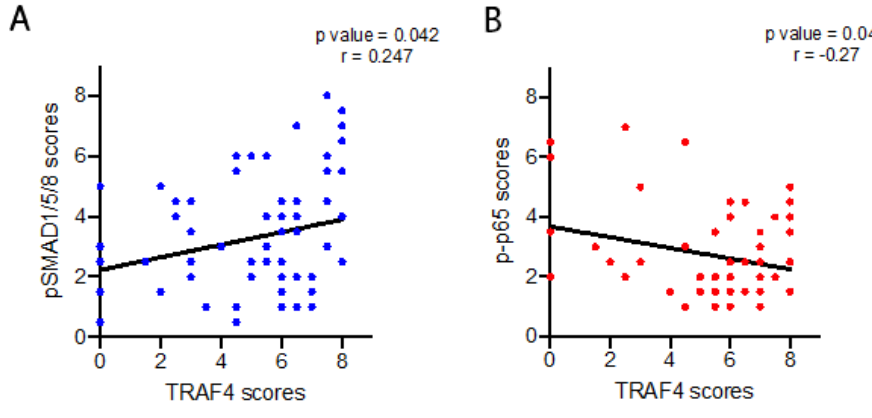

> Figure 7. TRAF4 expression correlates positively with pSMAD1/5/8 levels and negatively with the p-p65 level in bladder tumors

(A) Regression analysis showing the correlations between the TRAF4 expression level (score) and phospho (p)SMAD1/5/8 scores in bladder cancer patients. Pearson's chi-squared test was used to determine the correlations between the TRAF4 and pSMAD1/5/8 scores. **(B)** Regression analysis showing the correlations between the TRAF4 expression level (score) and phospho (p)-p65 score in bladder cancer patients. Pearson's chi-squared test was used to determine the correlations between the TRAF4 and p-p65 scores. **(C)** Representative images of continuous sections of tissue microarray samples probed with the indicated antibodies using fluorescent immunohistochemistry. The magnified insets for pSMAD1/5/8 show nuclear staining. Scale bar: 400 mm. **(D)** Schematic representation of TRAF4 signaling dynamics in epithelial-like and mesenchymal-like bladder cancer cells. Ub denotes ubiquitin and P stands for phosphorylation of serine 334.

Discussion

In this study, we investigated the role of TRAF4 during bladder cancer progression and in contrast to other cancer types, observed strong positive correlations between its expression and increased overall patient survival. Mining of publicly available data and our own analysis of experimental immunohistochemical of patients samples revealed that TRAF4 expression gradually decreases as bladder cancer progresses. Pathologically, stage 2 and 3 bladder tumors are more aggressive than stage 1 tumors and have muscle invasiveness, and consistent with these characteristics, we observed higher TRAF4 levels in stage 1 tumors. Furthermore, in both cultured cells and material from bladder cancer patients, we observed strong links between TRAF4 expression and increased BMP/SMAD and decreased NF-κB pathway signaling. Mechanistically, we showed that TRAF4 ubiquitinates and degrades SMURF1, a pro-EMT and oncogenic protein. TRAF4 directly and indirectly promotes BMP/SMAD signaling. Our results give credence to the claim that the interplay between TRAF4 and SMURF1 expression levels and activity functions as an important functional node in the interactions that enhance BMP/SMAD and NF-kb signaling crosstalk during bladder cancer progression (Figure 7D).

Epithelial-mesenchymal transition is a prominent event during bladder cancer metastasis, especially in bladder carcinoma, where (epithelial) cancer cells usually have to gain mesenchymal properties to penetrate through the bladder muscle wall. Mesenchymal markers *FN1* and *ITGAV* have been well documented as potential biomarkers or targets for bladder carcinoma[33,34]. Interestingly, we found a strong correlation between the EMT status of bladder cancer cells and TRAF4 expression. Knocking down TRAF4 in the epithelial cell line RT4 led to loose attachment of cells to colonies, suggesting possible loss of epithelial tight junction components. Physiologically, bladder urothelial cells have high expression of TRAF4, which perhaps enables the bladder to maintain a strong barrier against leakage of stored urine. Changes in the expression of the EMT transcription factors SNAIL and SLUG were observed upon TRAF4 knockdown. For example, in RT4 cells, there was an increase in SLUG and a decrease in SNAIL, and *vice versa* in HT1376 cells. This mutually exclusive expression pattern was observed across 5 bladder cancer cell lines used in this study, suggesting a certain level of functional redundancy or compensation. Indeed, such reciprocal effects of SNAIL and SLUG expression have been previously documented[35].

We investigated why the steady-state TRAF4 level is lower in mesenchymal bladder cells than in epithelial bladder cancer cells. Epigenetic repression of genes is commonly seen during cancer progression and is mediated by DNA methylation enzymes that methylate certain regions in promoters to diminish their transcriptional activity[36]. Treatment of mesenchymal bladder cell lines with 5-AZA, a compound that blocks DNA methylation, rescued *TRAF4* expression. This suggests that *TRAF4* is (directly or indirectly) epigenetically repressed. Our results also showed that the TRAF4 protein is less stable in more aggressive mesenchymal bladder cancer cells. We found that ERK-induced phosphorylation of TRAF4 mediates the decreases in the steady-state TRAF4 protein level and TRAF4 stability. Many of these aggressive (bladder) cancer cells have mutations in components of MAPK pathways, such as Raf or Ras, that increase the activity of downstream ERK signaling[10,11].

In this study, we observed that TRAF4 affected the SMURF1 protein level in bladder cancer cells; TRAF4 maintained an appropriate SMURF1 level, and as the TRAF4 level decreased, the steady-state SMURF1 level increased. We previously reported that TRAF4 is able to ubiquitinate SMURF2, thereby potentiating the TGF-β signaling and promoting breast cancer metastasis[14]TRAF4 is recruited to the active TGF-β receptor complex, where it antagonizes E3 ligase SMURF2 and facilitates the recruitment of deubiquitinase USP15 to the TGF-β type I receptor (TβRI. SMURF1 has high sequence similarity to SMURF2 and belongs to the same E3 ubiquitin ligase subfamily (HECT domain, NEDD4 subgroup). TRAFF4 has been reported to promote BMP signaling neural crest development and neural plate morphogenesis through SMURF1 inhibition[13]. BMP is a family member of TGF-β, which inhibits TGF- β-induced EMT and promotes mesenchymal to epithelial transition (MET). Additionally, there have been other important studies reflecting the dynamic interplay between TRAF4 and SMURF1[13,37]. Our observations reveal that upregulation of SMURF1 due to reduced TRAF4 expression in later stages of bladder cancer progression could indeed potentially dampen the BMP signaling output.

Whereas TRAF4 knockdown in epithelial bladder cancer cells promotes migration and induces loss of epithelial integrity, ectopic expression of TRAF4 in mesenchymal cells inhibits migration and invasion. Consistent with these observations, we found that exogenous addition of BMP ligand or a SMURF1 inhibitor (A01) to mesenchymal cells inhibited their migration. The latter compound inhibits the degradation of the BMP signaling pathway components

SMAD1 and SMAD5 by SMURF1. These data are in line with the hypothesis that TRAF4, by inhibiting SMURF1, potentiates BMP/SMAD signaling and thereby inhibits bladder cancer cell migration.

We performed unbiased transcriptomic and pathway analyses, which underlined our findings that TRAF4 promotes BMP signaling, and revealed that TRAF4 inhibits NF-κB signaling pathway activity in bladder cells. In contrast to other TRAF family members that mediate NF-κb signaling, TRAF4 has been shown to counteract other TRAF members and to antagonize NF-κb signaling. This is in line with our findings. NF-κb signaling was found to promote EMT and to play a role in bladder cancer progression[38].

The correlation of TRAF4 with BMP and NF-kb signaling pathways were confirmed in material from bladder cancer patients; Phosphorylated SMAD1/5 levels, indicative of active BMP receptor signaling, were found to be positively associated with high TRAF4 expression, while higher levels of phosphorylated NF-κb -p65 were associated with lower TRAF4 expression. This is consistent with our finding that TRAF4 targets SMURF1, for proteasomal degradation[39–41]. The negative correlation of TRAF4 with NF-κb gene response signature and NF-kb -p-p65 in patient samples is in line with our *in vitro* findings. Moreover, we observed that TNFα, an upstream activator of the NF-κB pathway, can diminish the BMP signaling output, and that this effect that can be reduced by TRAF4. The link of SMURF1 and TRAF4-induced inhibition of NF-κb have been identified previously [42]Runx2, RhoA and MEKK2 for ubiquitination and degradation. In a yeast two-hybrid screening, we identified TNF receptor-associated factor 4 (TRAF4. Taken together, these and our studies demonstrate the intimate crosstalk between TRAF4 and SMURF1 in regulating BMP/SMAD and NF-κb signaling.

In summary, we identified TRAF4 expression level as a key determinant in the progression of bladder cancer. We uncovered that TRAF4 has a negative role in this process by enhancing BMP/SMAD and inhibiting NF-κb signaling Low TRAF4 expression may be useful as a biomarker to detect aggressive types of bladder cancer. In future studies, it may be interesting to explore therapeutic potential of SMURF1 inhibitors or other BMP agonists in bladder cancer treatment.

Acknowledgments

We are grateful to Slobodan Vukicevics (University of Zagreb) for providing BMP6. We thank Midory Thorikay and Gerard van der Zon for technical assistance and Martijn Rabelink for the shRNA constructs. The MBT-2 cell line was a kind gift from Simon Dovedi. RNA-seq was performed by BGI Tech (Hong Kong). Karien Wiesmeijer and Annelies Boonzaier-van der Laan helped with scanning the tissue microarray slides. We also thank Kees Fluiter for providing advice on the pathway studies.

References

1. Siegel, R. L., Miller, K. D. & Jemal, A. Cancer statistics, 2020. CA. Cancer J. Clin. **70**, 7–30 (2020).
2. Lim, J. & Thiery, J. P. Epithelial-mesenchymal transitions: insights from development. Development **139**, 3471–3486 (2012).
3. Polyak, K. & Weinberg, R. A. Transitions between epithelial and mesenchymal states: acquisition of malignant and stem cell traits. Nat Rev Cancer **9**, 265–273 (2009).
4. Wheelock, M. J., Shintani, Y., Maeda, M., Fukumoto, Y. & Johnson, K. R. Cadherin switching. J Cell Sci **121**, 727–735 (2008).
5. Nieto, M. A., Huang, R. Y., Jackson, R. A. & Thiery, J. P. Emt: 2016. Cell **166**, 21–45 (2016).
6. Yang, J. et al. Guidelines and definitions for research on epithelial–mesenchymal transition. Nature Reviews Molecular Cell Biology vol. 21 341–352 (2020).
7. Hao, Y., Baker, D. & Dijke, P. Ten. TGF-β-mediated epithelial-mesenchymal transition and cancer metastasis. International Journal of Molecular Sciences vol. 20 2767 (2019).
8. Glaser, A. P., Fantini, D., Shilatifard, A., Schaeffer, E. M. & Meeks, J. J. The evolving genomic landscape of urothelial carcinoma. Nat Rev Urol **14**, 215–229 (2017).
9. Bekele, R. T. et al. RAF1 amplification drives a subset of bladder tumors and confers sensitivity to MAPK-directed therapeutics. J Clin Invest **131**, (2021).
10. Sim, W. J. et al. c-Met activation leads to the establishment of a TGFβ-receptor regulatory network in bladder cancer progression. Nat. Commun. 2019 101 **10**, 1–19 (2019).
11. Janda, E. et al. Ras and TGF[beta] cooperatively regulate epithelial cell plasticity and metastasis: dissection of Ras signaling pathways. J Cell Biol **156**, 299–313 (2002).
12. Park, H. H. Structure of TRAF Family: Current Understanding of Receptor Recognition. Front. Immunol. **9**, (2018).
13. Kalkan, T., Iwasaki, Y., Park, C. Y. & Thomsen, G. H. Tumor necrosis factor-receptor-associated factor-4 is a positive regulator of transforming growth factor-beta signaling that affects neural crest formation. Mol Biol Cell **20**, 3436–3450 (2009).
14. Zhang, L. et al. TRAF4 promotes TGF-beta receptor signaling and drives breast cancer metastasis. Mol Cell **51**, 559–572 (2013).
15. Singh, R. et al. TRAF4-mediated ubiquitination of NGF receptor TrkA regulates prostate cancer metastasis. J Clin Invest **128**, 3129–3143 (2018).
16. Kim, E. et al. TRAF4 promotes lung cancer aggressiveness by modulating tumor microenvironment in normal fibroblasts. Sci Rep **7**, 8923 (2017).
17. Li, W. et al. TRAF4 is a critical molecule for Akt activation in lung cancer. Cancer Res **73**, 6938–6950 (2013).
18. Liu, Y., Duan, N. & Duan, S. MiR-29a Inhibits Glioma Tumorigenesis through a Negative Feedback Loop of TRAF4/Akt Signaling. Biomed Res Int **2018**, 2461363 (2018).
19. Tan, T. Z., Rouanne, M., Tan, K. T., Huang, R. Y. J. & Thiery, J. P. Molecular Subtypes of Urothelial Bladder Cancer: Results from a Meta-cohort Analysis of 2411 Tumors. Eur. Urol. **75**, 423–432 (2019).
20. Tan, T. Z. et al. Epithelial-mesenchymal transition spectrum quantification and its efficacy in deciphering survival and drug responses of cancer patients. EMBO Mol Med **6**, 1279–1293 (2014).
21. Earl, J. et al. The UBC-40 Urothelial Bladder Cancer cell line index: a genomic resource for functional studies. BMC Genomics **16**, 403 (2015).
22. Wu, K. et al. Slug contributes to cadherin switch and malignant progression in muscle-invasive bladder cancer development. Urol Oncol **31**, 1751–1760 (2013).
23. Stadler, M. et al. Exclusion from spheroid formation identifies loss of essential cell-cell adhesion molecules in colon cancer cells. Sci Rep **8**, 1151 (2018).
24. Smyrek, I. et al. E-cadherin, actin, microtubules and FAK dominate different spheroid formation phases and important elements of tissue integrity. Biol Open **8**, (2019).
25. Wang, H. R. et al. Degradation of RhoA by Smurf1 ubiquitin ligase. Methods Enzym. **406**, 437–447 (2006).
26. Sahai, E., Garcia-Medina, R., Pouyssegur, J. & Vial, E. Smurf1 regulates tumor cell plasticity and motility through degradation of RhoA leading to localized inhibition of contractility. J Cell Biol **176**, 35–42 (2007).
27. Kalkan, T., Iwasaki, Y., Chong, Y. P. & Thomsen, G. H. Tumor necrosis factor-receptor-associated factor-4 is a positive regulator of transforming growth factor-beta signaling that affects neural crest formation. Mol. Biol. Cell **20**, 3436–3450 (2009).
28. Cao, Y. et al. Selective Small Molecule Compounds Increase BMP-2 Responsiveness by Inhibiting Smurf1-mediated Smad1/5 Degradation. Sci. Reports 2014 41 **4**, 1–11 (2014).
29. Cao, Y. et al. Selective small molecule compounds increase BMP-2 responsiveness by inhibiting Smurf1-mediated Smad1/5 degradation. Sci Rep **4**, 4965 (2014).
30. Takeshita, F. et al. TRAF4 acts as a silencer in TLR-mediated signaling through the association with TRAF6 and TRIF. Eur J Immunol **35**, 2477–2485 (2005).
31. Hollnagel, A., Oehlmann, V., Heymer, J., Ruther, U. & Nordheim, A. Id genes are direct targets of bone morphogenetic protein induction in embryonic stem cells. J Biol Chem **274**, 19838–19845 (1999).
32. Takase, M. et al. Induction of Smad6 mRNA by bone morphogenetic proteins. Biochem Biophys Res Commun **244**, 26–29 (1998).
33. Yang, X. et al. Diagnostic value of bladder tumor fibronectin in patients with bladder tumor: a systematic review with meta-analysis. Clin Biochem **46**, 1377–1382 (2013).
34. van der Horst, G. et al. Targeting of alpha-v integrins reduces malignancy of bladder carcinoma. PLoS One **9**, e108464 (2014).

35. Nakamura, R. et al. Reciprocal expression of Slug and Snail in human oral cancer cells. PLoS One **13**, e0199442 (2018).
36. Suriyamurthy, S., Baker, D., Ten Dijke, P. & Iyengar, P. V. Epigenetic Reprogramming of TGF-beta Signaling in Breast Cancer. Cancers (Basel) **11**, (2019).
37. Wang, X., Jin, C., Tang, Y., Tang, L. Y. & Zhang, Y. E. Ubiquitination of tumor necrosis factor receptor-associated factor 4 (TRAF4) by Smad ubiquitination regulatory factor 1 (Smurf1) regulates motility of breast epithelial and cancer cells. J Biol Chem **288**, 21784–21792 (2013).
38. Wu, Q. et al. ROC1 promotes the malignant progression of bladder cancer by regulating p-IκBα/NF-κB signaling. J. Exp. Clin. Cancer Res. **40**, 1–13 (2021).
39. Zhu, H., Kavsak, P., Abdollah, S., Wrana, J. L. & Thomsen, G. H. A SMAD ubiquitin ligase targets the BMP pathway and affects embryonic pattern formation. Nature **400**, 687–693 (1999).
40. Ying, S. X., Hussain, Z. J. & Zhang, Y. E. Smurf1 facilitates myogenic differentiation and antagonizes the bone morphogenetic protein-2-induced osteoblast conversion by targeting Smad5 for degradation. J Biol Chem **278**, 39029–39036 (2003).
41. Murakami, G., Watabe, T., Takaoka, K., Miyazono, K. & Imamura, T. Cooperative inhibition of bone morphogenetic protein signaling by Smurf1 and inhibitory Smads. Mol Biol Cell **14**, 2809–2817 (2003).
42. Li, S. et al. Ubiquitin ligase Smurf1 targets TRAF family proteins for ubiquitination and degradation. Mol. Cell. Biochem. **338**, 11–17 (2010).
43. Yung, Y., Yao, Z., Aebersold, D. M., Hanoch, T. & Seger, R. Altered regulation of ERK1b by MEK1 and PTP-SL and modified Elk1 phosphorylation by ERK1b are caused by abrogation of the regulatory C-terminal sequence of ERKs. J. Biol. Chem. **292**, 8852 (2017).
44. Irshad, S. et al. Bone morphogenetic protein and Notch signalling crosstalk in poor-prognosis, mesenchymal-subtype colorectal cancer. J. Pathol. **242**, 178–192 (2017).
45. Stolpe, A. van de, Holtzer, L., van Ooijen, H., de Inda, M. A. & Verhaegh, W. Enabling precision medicine by unravelling disease pathophysiology: quantifying signal transduction pathway activity across cell and tissue types. Sci. Rep. **9**, (2019).
46. Jones, G., Willett, P., Glen, R. C., Leach, A. R. & Taylor, R. Development and validation of a genetic algorithm for flexible docking. J. Mol. Biol. **267**, 727–748 (1997).

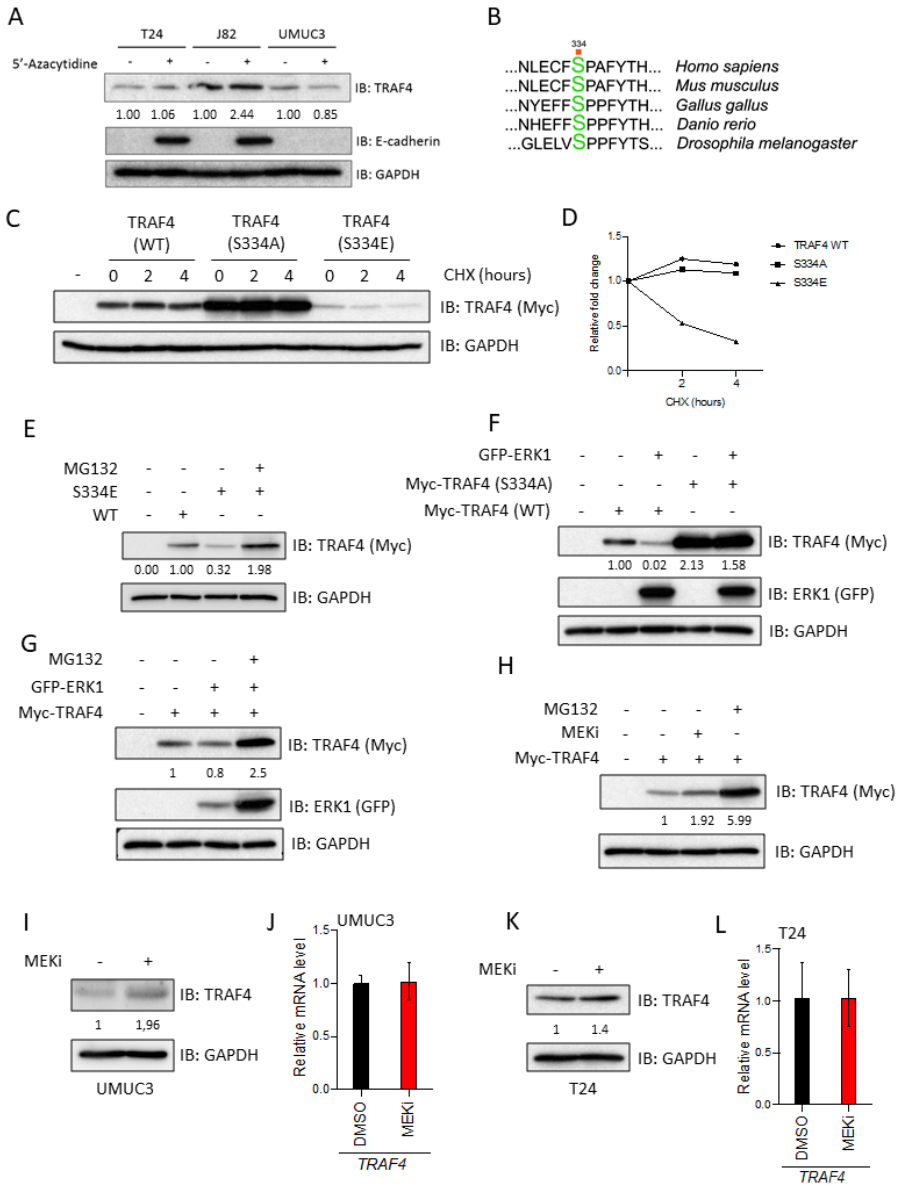

< Figure S1

(A) Immunoblot analysis with the indicated antibodies in cell lines treated with either control (DMSO) or 5-azacitidine; GAPDH, loading control. The numbers indicate the relative quantitative TRAF4 levels with respect to the loading control GAPDH. **(B)** Multiple sequence alignment indicating the conservation of serine 334 of TRAF4 in different species. **(C)** Immunoblot results from 293T cells transfected with wild-type, S334A mutant or S334E mutant TRAF4; cells were treated with cycloheximide (CHX, 10 μg/ml) for the indicated times and lysed. **(D)** Graph of C showing the rate of degradation of proteins with respect to the loading control GAPDH. **(E)** Immunoblot results from 293T cells transfected with the indicated plasmids. The proteasome inhibitor MG132 was added overnight at a concentration of 2 μM. GAPDH, loading control. The numbers indicate the relative quantitative TRAF4 levels with respect to the loading control GAPDH. **(F)** Immunoblot analysis of 293T cells transfected with the indicated plasmids; GAPDH, loading control. **(G)** Immunoblot analysis of 293T cells transfected with the indicated plasmids. MG132 was added overnight at a 2 μM concentration where indicated. GAPDH, loading control. **(H)** Immunoblot analysis of 293T cells transfected with Myc-TRAF4; MG132 or the MEK inhibitor (MEKi; PD0325901) was added overnight at a concentration of 2 μM as indicated. The numbers indicate the relative quantitative TRAF4 levels with respect to the loading control GAPDH. **(I)** Immunoblot analysis of UMUC3 cells treated overnight with the MEKi at a concentration of 2 μM as indicated; the numbers indicate the relative levels of TRAF4. GAPDH, loading control. **(J)** Real-time PCR analysis of TRAF4 mRNA expression after treating cells with the MEKi overnight as indicated; the error bars indicate ± SD. **(K)** Immunoblot analysis of T24 cells treated overnight with the MEKi at a concentration of 2 μM as indicated; the numbers indicate the relative levels of TRAF4 with respect to GAPDH. GAPDH, loading control. **(L)** Real-time PCR analysis of TRAF4 mRNA expression after treating cells with the MEKi overnight as indicated.

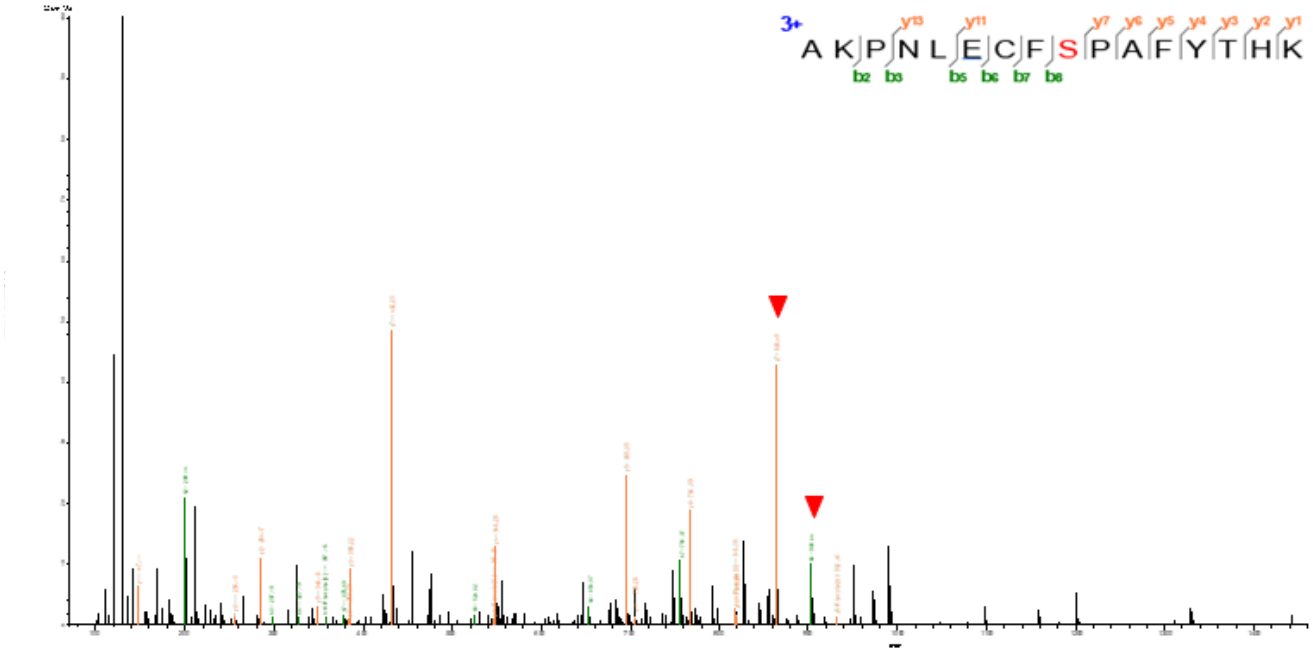

Sequence: AKPNLECFSPAFYTHK, S9-Phospho (79.96633 Da)
Charge: +3, Monoisotopic m/z: 644.96210 Da (+0.11 mmu/+0.18 ppm), MH+: 1932.87174 Da, RT: 56.6833 min,
Identified with: Mascot (v1.36); Ions Score:26, Percolator q-Value:0, Percolator PEP:0.00264, Ions matched by search engine: 9/176
Fragment match tolerance used for search: 50 mmu

Figure S2
Mass Spectrometry spectra identifying TRAF4 S334 phosphorylation sites. FLAG-TRAF4 expressed by 293T was immunoprecipitated and subjected to mass spectrometry. Shown is the peptide sequence AKPNLECFSPAFYTHK, including S334. Mascot (v1.36) was used for identification.

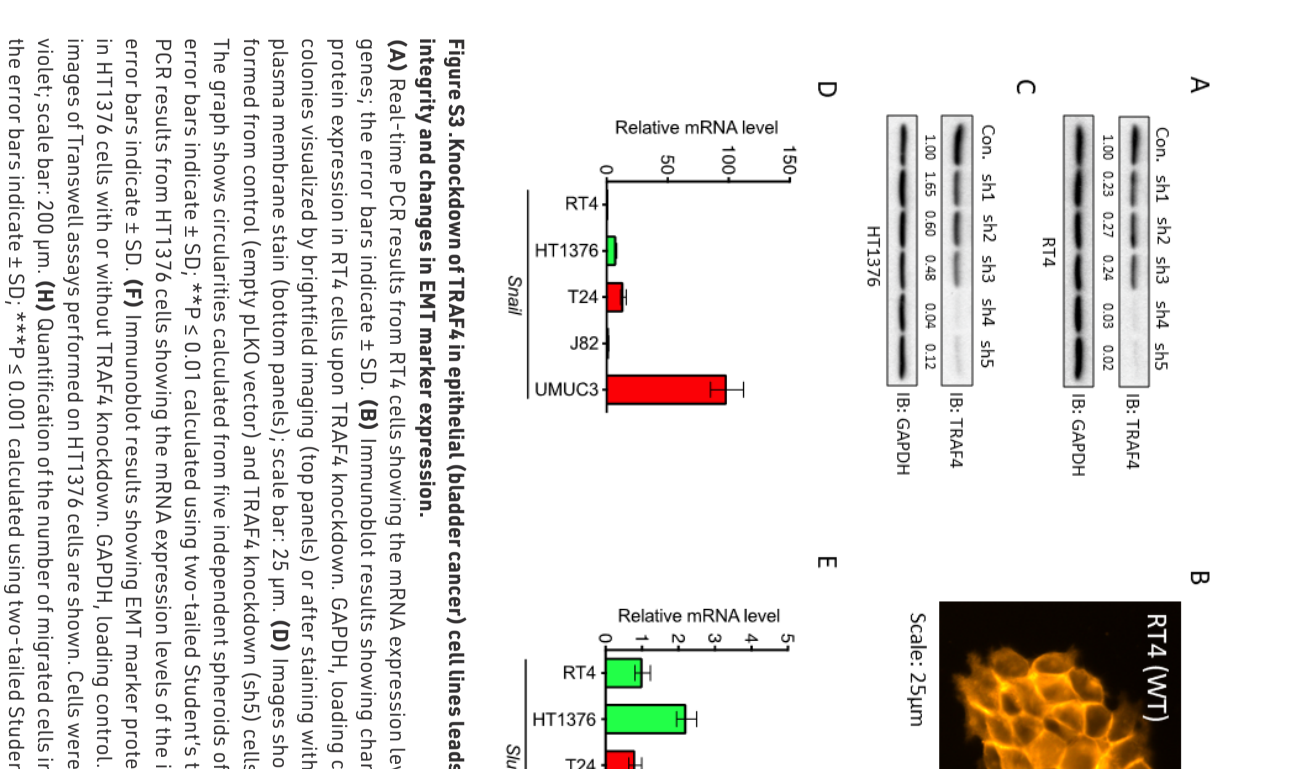

Figure S3 .Knockdown of TRAF4 in epithelial (bladder cancer) cell lines leads to loss of epithelial integrity and changes in EMT marker expression.
(A) Real-time PCR results from RT4 cells showing the mRNA expression levels of the indicated genes; the error bars indicate ± SD. **(B)** Immunoblot results showing changes in EMT marker protein expression in RT4 cells upon TRAF4 knockdown. GAPDH, loading control. **(C)** RT4 cell colonies visualized by brightfield imaging (top panels) or after staining with CellMask™ Orange plasma membrane stain (bottom panels); scale bar: 25 μm. **(D)** Images showing RT4 spheroids formed from control (empty pLKO vector) and TRAF4 knockdown (sh5) cells; scale bar: 200 μm. The graph shows circularities calculated from five independent spheroids of different sizes. The error bars indicate ± SD; $^{**}P \leq 0.01$ calculated using two-tailed Student's t test. **(E)** Real-time PCR results from HT1376 cells showing the mRNA expression levels of the indicated genes; the error bars indicate ± SD. **(F)** Immunoblot results showing EMT marker protein expression levels in HT1376 cells with or without TRAF4 knockdown. GAPDH, loading control. **(G)** Representative images of Transwell assays performed on HT1376 cells are shown. Cells were stained with crystal violet; scale bar: 200 μm. **(H)** Quantification of the number of migrated cells in four random fields; the error bars indicate ± SD; $^{***}P \leq 0.001$ calculated using two-tailed Student's t test.

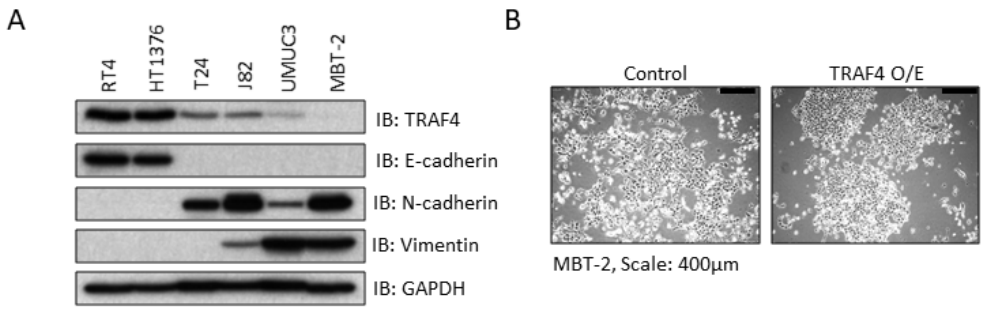

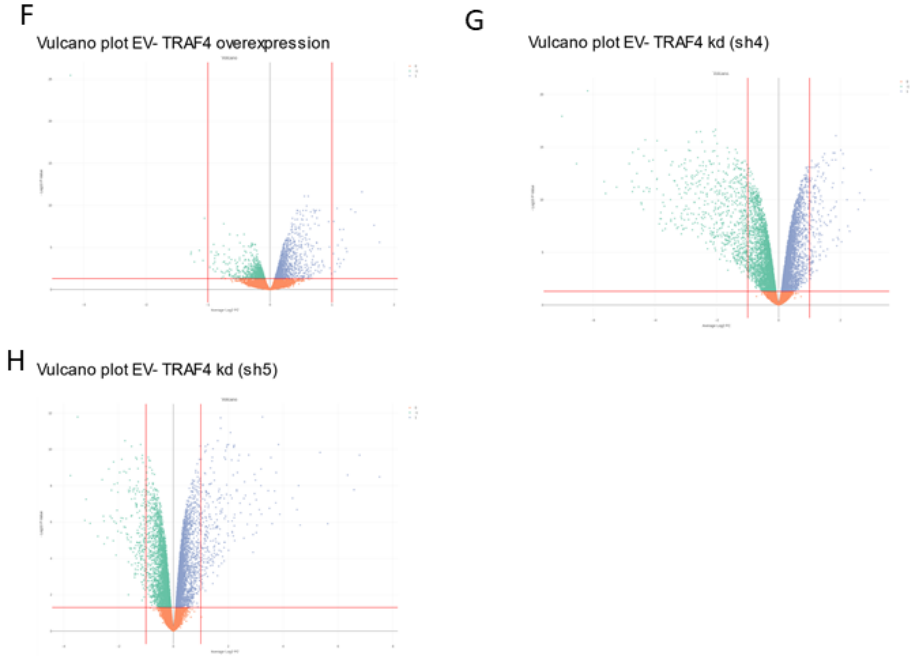

< Figure S4

(A) Immunoblot analysis showing the expression of TRAF4 and other EMT marker proteins in bladder cancer cell lines, including MBT-2. GAPDH, loading control. **(B)** Brightfield images of MBT-2 (control and TRAF4-overexpressing) cells seeded and grown at a low density; scale bar: 400 μm (representative images). **(C)** Immunoblot results showing the Smurf1 level in MBT-2 cells stably expressing either control (empty pLKO vector) or SMURF1 shRNAs. GAPDH, loading control. **(D)** Real-time PCR results showing the mRNA expression of SMURF2 using SMURF1 knockdown constructs sh1 and sh2, corrected for GAPDH expression. The error bars indicate ± SD. **(E)** Immunoblot analysis of T24 cells stably expressing TRAF4. A-D are the four replicates used for transcriptome analysis. GAPDH, loading control.

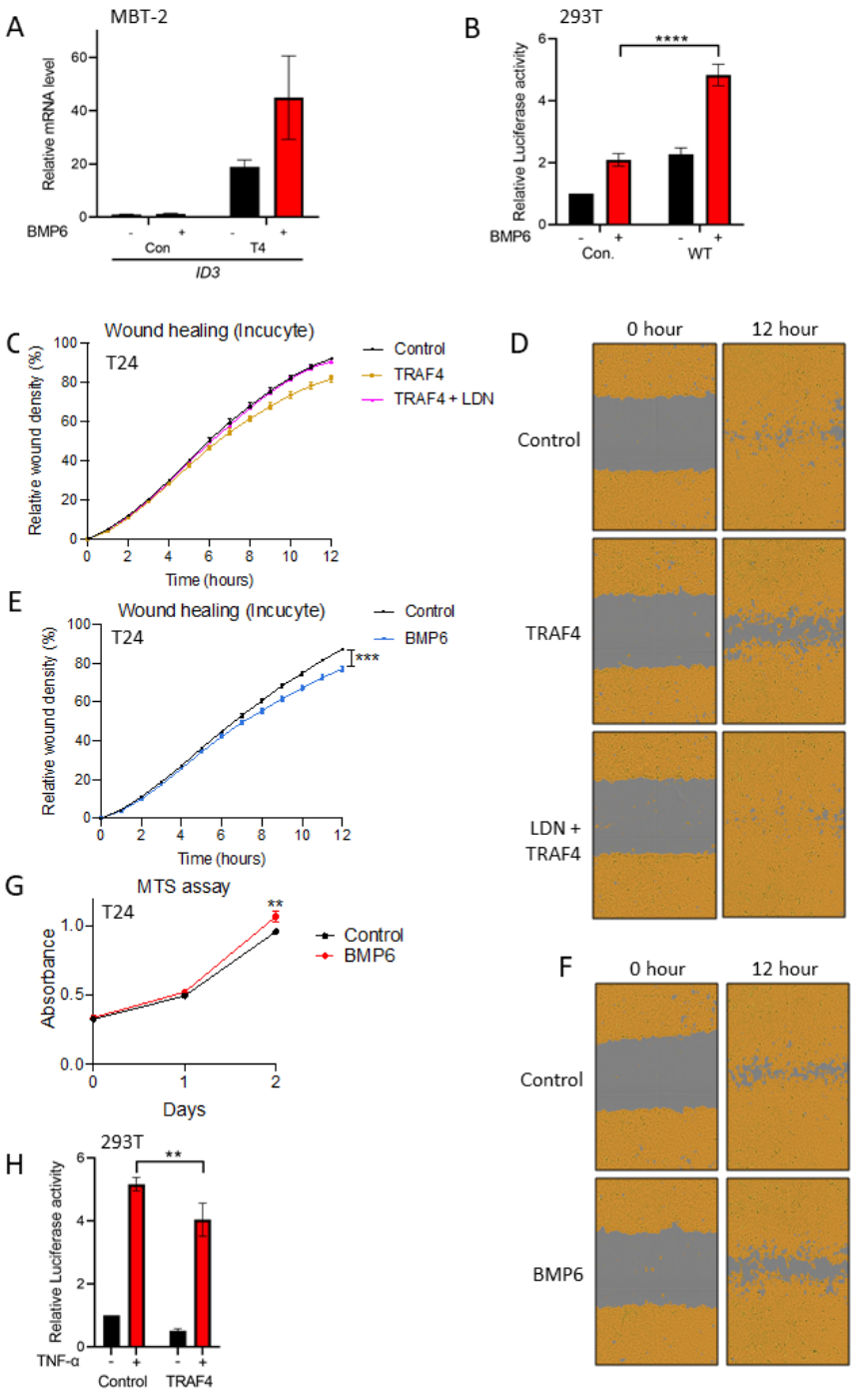

< Figure S5

(A) Real-time PCR results showing the ID3 mRNA expression level in BMP6 (50 ng/ml for 2 hours)-treated control or TRAF4-overexpressing (T4) MBT-2 cells as indicated; the error bars indicate ± SD. **(B)** Luciferase reporter assay in 293T cells transfected with the BRE-luciferase reporter, SV40 Renilla and either empty vector control or TRAF4. Transfected cells were stimulated overnight with BMP6 (50 ng/ml) where indicated. The error bars indicate ± SD; ****P ≤ 0.0001 calculated using two-way ANOVA. **(C)** Graph showing the relative wound widths in T24 cells as determined with an IncuCyte system. TRAF4-overexpressing cells were treated with the selective BMP type I receptor kinase inhibitor LDN193189 at a concentration of 120 nM where indicated. Images were acquired every hour after the wound was produced; the error bars indicate ± SEM. **(D)** Representative images from the IncuCyte® experiment shown in **(C)**. The brown area represents the cell coverage, and the gray area indicates the original wound produced and the remaining wound. **(E)** Graph showing the relative wound widths as determined with an IncuCyte® system. Images were acquired every hour after the wound was produced. T24 cells were treated with BMP6 (50 ng/ml); the error bars indicate ± SEM; ***P ≤ 0.001 calculated using two-tailed Student's t test. **(F)** Representative images from the experiment in G. The brown area represents the cell coverage, and the gray area indicates the wound produced and the remaining wound. **(G)** An MTS assay was performed with T24 cells either untreated or stimulated with BMP6 (50 ng/ml). The absorbance was measured at the indicated time points; the error bars indicate ± SD from three sample replicates; **P ≤ 0.01 calculated using two-tailed Student's t test. **(H)** Luciferase assay in 293T cells transfected with the NF-*k*B luciferase reporter, SV40 Renilla and either empty vector control or TRAF4. Transfected cells were stimulated overnight with TNF-*α* (10 ng/ml) where indicated. The error bars indicate ± SD; **P ≤ 0.01, calculated using two-tailed two-way ANOVA. Representative results from three independent experiments are shown.